FLECS_WT3.1_3.3_3.4_TN
https://doi.org/10.48441/4427.2052

Hochschule für Angewandte Wissenschaften Hamburg
Hamburg University of Applied Sciences

Functional Model Library of the Environmental Control Systems (FLECS) – Physical Description

Preliminary Investigations of ECS-Modeling
Modeling of Subsystems
Documentation of the Mathematical Description

Christian Müller
Dieter Scholz

2008-03-07

Technical Note

Aircraft Design and Systems Group (AERO)
Department of Automotive and Aeronautical Engineering
Hamburg University of Applied Sciences (HAW Hamburg)
Berliner Tor 9
D - 20099 Hamburg

Dokumentationsblatt

1. Berichts-Nr. FLECS_WT3.1_3.3_3.4_TN	**2. Auftragstitel** FLECS - Funktionale Modellbibliothek des Environmental Control Systems	**3. ISSN / ISBN** ---
4. Sachtitel und Untertitel (Work Tasks) WT3.1: Voruntersuchungen zur Modellbildung WT3.3: Modellierung der Subsysteme WT3.4: Dokumentation der mathematischen Beschreibung		**5. Abschlußdatum** 07.03.2008 **6. Ber. Nr. Auftragnehmer** ---
7. Autor(en) (Vorname, Name) Christian Müller Dieter Scholz (info@ProfScholz.de)		**8. Vertragskennzeichen** HH59 **9. Projektnr.** FLAND05-006
10. Durchführende Institution (Name, Anschrift) Aircraft Design and Systems Group (AERO) Department Fahrzeugtechnik und Flugzeugbau Hochschule für Angewandte Wissenschaften Hamburg (HAW Hamburg) Berliner Tor 9, D - 20099 Hamburg		**11. Berichtsart** Technische Niederschrift **12. Berichtszeitraum** 05.09.2005 - 15.03.2008 **13. Seitenzahl** 69
14. Fördernde Institution / Projektträger (Name, Anschrift) Behörde für Wirtschaft und Arbeit (BWA) Alter Steinweg 4, D - 20459 Hamburg Deutsches Zentrum für Luft- und Raumfahrt e.V. (DLR), PT-LF Königswinterer Straße 522-524, D - 53227 Bonn		**15. Literaturangaben** 23 **16. Tabellen** 15 **17. Bilder** 37
18. Zusätzliche Angaben Sprache: Englisch URL: http://FLECS.ProfScholz.de		
19. Kurzfassung Innerhalb des FLECS Projekts soll eine Datenbank für die System Sim ulation des Enviromental Control System (ECS) erstellt werden. Jeder Komponente des ECS wird ein Simulink Funktionsblock zugeordnet. Allgemein beschränkt sich die Beschreibung der ECS auf die Beschreibung der Luft/ Gassysteme. Jedem Funktionsblock liegt ein physikalisches Model zu Grunde, dass das reale Verhalten der Kom ponenten beschreibt. Die entwickelten Modelle werden so allgem eingültig wie möglich definiert und beachten thermodynamische und strömungsmechanische Grundlagen für. • Allgemeine Volumenblöcke mit Luftfeuchte beachten CO_2-Gehalt und flüssiges Wasser, • Kondensations- und Verdampfungsprozesse, • inkompressible und kompressible Strömungen. Weitere Elemente sind: • Strömungsknoten, • Wärmeübergangselemente, • statische und dynamische Wärmetauscher, • spezielle Strömungselemente wie z.B. Kompressor und Turbine, • Kaltdampfklimasysteme.		
20. Deskriptoren / Schlagwörter Flugzeug, System, Klimaanlage, Kabine, Simulation, Modellbibliothek, MATLAB, Simulink		
21. Bezugsquelle Studiendepartment F+F, HAW Hamburg, Berliner Tor 9, D - 20099 Hamburg		
22. Sicherheitsvermerk öffentlich	**23.**	**24. Preis**

Report Documentation Page

<table>
<tr><td>1. Report-Number
FLECS_WT3.1_3.3_3.4_TN</td><td>2. Project Title
FLECS - Functional Model Library of the Environmental Control System</td><td>3. ISSN / ISBN
N/A</td></tr>
<tr><td colspan="2" rowspan="2">4. Title and Subtitle (Work Tasks)
WT3.1: Preliminary Investigations of ECS-Modeling
WT3.3: Modeling of Subsystems
WT3.4: Documentation of the Mathematical Description</td><td>5. Report Date
2008-03-07</td></tr>
<tr><td>6. Performing Org. Rep. No
N/A</td></tr>
<tr><td colspan="2" rowspan="2">7. Author(s) (First Name, Last Name)
Christian Müller
Dieter Scholz (info@ProfScholz.de)</td><td>8. Contract Code
HH59</td></tr>
<tr><td>9. Project Number
FLAND05-006</td></tr>
<tr><td colspan="2" rowspan="3">10. Performing Agency (Name, Address)
Aircraft Design and Systems Group (AERO)
Department of Automotive and Aeronautical Engineering
Hamburg University of Applied Sciences (HAW Hamburg)
Berliner Tor 9, D - 20099 Hamburg</td><td>11. Report Type
Technical Note</td></tr>
<tr><td>12. Time Period
2005-09-05 to 2008-03-15</td></tr>
<tr><td>13. Number of Pages
69</td></tr>
<tr><td colspan="2" rowspan="3">14. Sponsoring / Monitoring Agency (Name, Address)
Behörde für Wirtschaft und Arbeit (BWA)
Alter Steinweg 4, D - 20459 Hamburg

Deutsches Zentrum für Luft- und Raumfahrt e.V. (DLR), PT-LF
Königswinterer Straße 522-524, D - 53227 Bonn</td><td>15. Number of References
23</td></tr>
<tr><td>16. Number of Tables
15</td></tr>
<tr><td>17. Number of Figures
37</td></tr>
<tr><td colspan="3">18. Supplementary Notes
Language: English URL: http://FLECS.ProfScholz.de</td></tr>
<tr><td colspan="3">19. Abstract
The task of the FLECS project is the development of a database for the Environmental Control System (ECS). Each component of the ECS is related to one model block. In general the description of the ECS is correlated to the description of an air/gas distribution network. The model blocks correspond to a physical model. The inner structure of the models is built up as universal as possible considering thermodynamic and fluid mechanic basics.
Generalized volume elements consider water vapor, CO_2 content and free water,
condensation and evaporation processes,
incompressible and compressible flow conditions. Further elements:
Nodes,
heat transfer elements,
steady state and dynamical heat exchangers,
specialized flow resistances like compressors and turbines,
vapor compression cycle systems.</td></tr>
<tr><td colspan="3">20. Subject Terms
aircraft, system, air conditioning, ECS, cabin, simulation, model library, MATLAB, Simulink</td></tr>
<tr><td colspan="3">21. Distribution
Department F+F, HAW Hamburg, Berliner Tor 9, D - 20099 Hamburg</td></tr>
<tr><td>22. Classification / Availability
public / unlimited</td><td>23.</td><td>24. Price</td></tr>
</table>

Table of Contents

MATLAB/Simulink Model Library and Documentation available from:
https://doi.org/10.7910/DVN/US3KUY

List of Figures

List of Tables

List of Symbols

a	Sonic Speed	m/s
A	Surface	m^2
b	Thickness	m
c	Specific Heat Capacity	J/kg K
C	Heat Capacity	J/K
D	Diameter	m
E	Total Energy	J
h	Altitude	ft
	Specific Enthalpy	J/kg
H	Enthalpy	J
L	Length	m
m	Mass	kg
M	Mole Mass	g/mol
Ma	Mach Number	–
Nu	Nusselt Number	–
p	Pressure	Pa
P	Power	W
	Probability	–
Pr	Prandtl Number	–
r	Radius	m
	Ratio	–
R	Specific Gas Constant	J/kg K
Re	Reynolds Number	–
q	Heat Flux	J/m^2
Q	Heat	J
s	Specific Entropy	J/kg
S	Entropy	J
t	Time	s
T	Thermodynamically Temperature	K
u	Specific Intrinsic Energy	J/kg
U	Intrinsic Energy	J
v	Velocity	m/s
V	Volume	m^3
W	Work	J

x	Mass Fraction (Normalized to Mass Dry Air)	–
	Ratio	–
α	Convection Heat Transfer Coefficient	W/m^2 K
β	Angle	°
ε	Emissity	–
γ	Ratio Specific Heat Capacity	–
η	Dynamic Viscosity	Pa s
	Efficiency	–
φ	Humidity	–
κ	Compressibility	1/K
λ	Drag Coefficient	–
	Thermal Conductivity	W/m K
ν	Kinematic Viscosity	m^2/s
ρ	Density	kg/m^3
σ	Stefan Boltzmann constant	$5.67 \cdot 10^8$ J/s m^2 K
τ	Response Time	s
υ	Empirical Temperature	°C
ω	Angular Speed	°/s
ξ	Minor Loss Coefficient	–

Indices

0	Standard Condition
	Initial Condition
air	Dry air
CO2	CO_2
comp	Compressor
cond	Condensation
	Heat Conduction
conv	Heat Convection
corr	Corrected value
db	Dry Bulb
dar	Dry Air Rated
evap	Evaporation
H2O,gas	Water Vapor
H2O,liq	Free Water
hot	Hot Condition
in	Input Value
init	Initialization Value
inlet	Inlet of a Component
limit	Limit value
max	Maximum Value
min	Minimum Value
mix	Value of a mixed air flow
outlet	Outlet of a Component
p	Constant Pressure
v	Constant Volume
out	Output Value
s	Surface
sat	Saturation
trb	Turbine

List of Abbreviation

1D	One Dimension
	One Aperture
2D	Two Apertures
3D	Three Dimension
	Three Apertures
4D	Four Apertures
ACM	Air Cycle Machine
CFD	Computational Fluid Mechanics
CPU	Central Processing Unit
ECS	Environmental Control System
FLECS	Functional Model Library of the Environmental Control System
FR	Flow Resistance
HIL	Hardware in the Loop
ISA	International Standard Atmosphere
LCD	Light Crystal Display
NTU	Number of Transfer Units
PC	Personal Computer
SAT-COM	Satellite Communication
TN	Technical Note
TN_APP	Technical Note Applications
TN_PD	Technical Note Physical Description
VCC	Video Control Compartment
VCM	Vapor Cycle Machine

1 Introduction

Within the scope of the FLECS-project (FLECS: *Functional Model Library of the Environmental Control System*) a model-database should be developed, which enables the end-users to simulate the dynamical behavior of an Environmental Control System (ECS: *Environmental Control System*) .

Environmental control system: Heating, cooling, ventilation, distribution and purification of the air as well as control of temperature, pressure and humidity are the tasks of an environmental control system on board of air-crafts. Already in the early stage of the aircraft development different system architectures need to be compared. Trade studies need to be performed to evaluate system architecture against other alternatives, in order to be able to choose the most suitable one in the end. The many functions of an ECS require many components, which need to be sized and tuned to each other in an optimum way.

Simulation: The ECS development as just described is achieved today with the help of simulation. Three main areas of simulation in the ECS development may be differentiated:

- the calculation of three-dimensional (3D) flow fields in components of the environmental control system or the aircraft cabin by means of Computational Fluid Mechanics (CFD),
- the simulation of one-dimensional (1D) flow in air distribution networks,
- functional simulations of the environmental control system and the cabin.

The functional simulation is the topic of the project FLECS. It encompasses especially the description of thermodynamics, mechanics and control aspects of the ECS and its components with an emphasis on their dynamics and interaction.

Functional simulation is a mean to support the activities in all phases of the design and to track the development progress. To be supportive to the design process, the simulation activities shall be traceable and as seamless as possible. During early aircraft program concept phases there is the need to investigate a large number of potential system architectures in a short time frame with the help of simulation, to find the best candidates for an optimum architecture. After down selection of system architectures, simulation models need to be further detailed giving a better insight into the expected system behavior.

It shall be possible to enhance the simulation model used for concept studies by simply adding more detail without changing the architecture of the simulation model. During this detailing process the number of contributors to such a model is increasing, as more technical disciplines get deeply involved (e.g. thermodynamics group as well as controller design group).

To be compatible to such a process FLECS follows a strictly modular approach. Sub-components representing generic physical mechanisms or software functions are assembled to components, representing a piece of aircraft equipment or a certain controller function.

Components are grouped into component classes covering major aircraft functions to structure the resulting library. Components of the library are available in three different detail levels "Pre-Design", "Simple Dynamic" and "Detailed Dynamic", to cope with the different needs during different design phases. Interfaces of the components are standardized to ensure easy replacement of components with different detail levels.

If the design process enters the phase of prototypes, there is the need of product verification. For hardware in the loop (HIL) testing of controllers, simulated equipment is needed to close the loop. HIL testing takes place in a real-time environment, which needs real-time capable simulation models. Such models are integrated on the test rig as C-code, compiled and linked on the target platform. With the chosen simulation tool for FLECS, MATLAB/Simulink, C-Code can automatically be generated. To fulfill real time constraints for the generated C-Code, the user has to use components up to 'Simple Dynamic' level. In addition with a small set of overall modeling guidelines, the usage of these components ensures the later use of desktop models for HIL activities, without adding additional burden to the users of the library.

System designers have the need to use simulation models in two different ways: An interactive mode, where the model reacts to interactive user inputs. This is especially useful for design verification activities, when models are used to get a better insight of complex system behavior. On the other hand, there is a need to run a large number of predefined test cases in batch mode, to ensure proper system functionality in the whole operational envelope of the system.

Furthermore it needs to be ensured, that during system development already verified functions are still working properly (regression testing). Within the FLECS project interactive mode as well as batch mode functionality has been developed. As models get more and more complex during system development, simulation performance is an issue in a desktop environment. Surprisingly there are fewer performance constraints on HIL test rigs, because the modular structure of the model allows easy distribution of sub-model parts on to different processor cards.

A similar principle is applied to the desktop environment: Within the FLECS project, methods are developed to generate C-Code for sub-models, which include the numerical solver for the sub-model. Different integration step sizes are applied for the different sub-models. This approach results in an optimized use of CPU time, as every sub-model is solved with the most appropriate solver and time step. For future applications it is envisaged to run the sub-models on different CPUs, allowing the creation of comprehensive Software in the Loop test environment.

Innovative technologies in the area of ECS in aircrafts are e.g. bleedless aircraft, vapor cycle system, new control concepts, increase of cabin air humidity and galley cooling. These new technologies require standard components as well as new ones that are modeled in the FLECS project. In this way a functional ECS simulation is built up that ensures the safe introduction and integration of these new technologies in the aircraft.

Implementation of FLECS in the industrial process of environmental control system development: The development process of an aircraft environmental control system follows the widely used V-model. In general the V-model (see Figure 1) is associated with software development. Starting with the aircraft top level requirements, system requirements are derived to fulfill the aircraft top level requirements and to add the necessary level of detail for a complete specification of the respective system. The system specification process comprises three different levels of detail. High level system requirements, stating global system behavior in the aircraft context are followed by a functional system specification. The functional specification is a breakdown of all functions a system has to fulfill, without giving a solution how this function is to be implemented. The implementation down to signal level (for the software parts of a system) or down to a single piece of equipment (for the hardware parts) is described in the detail specification.

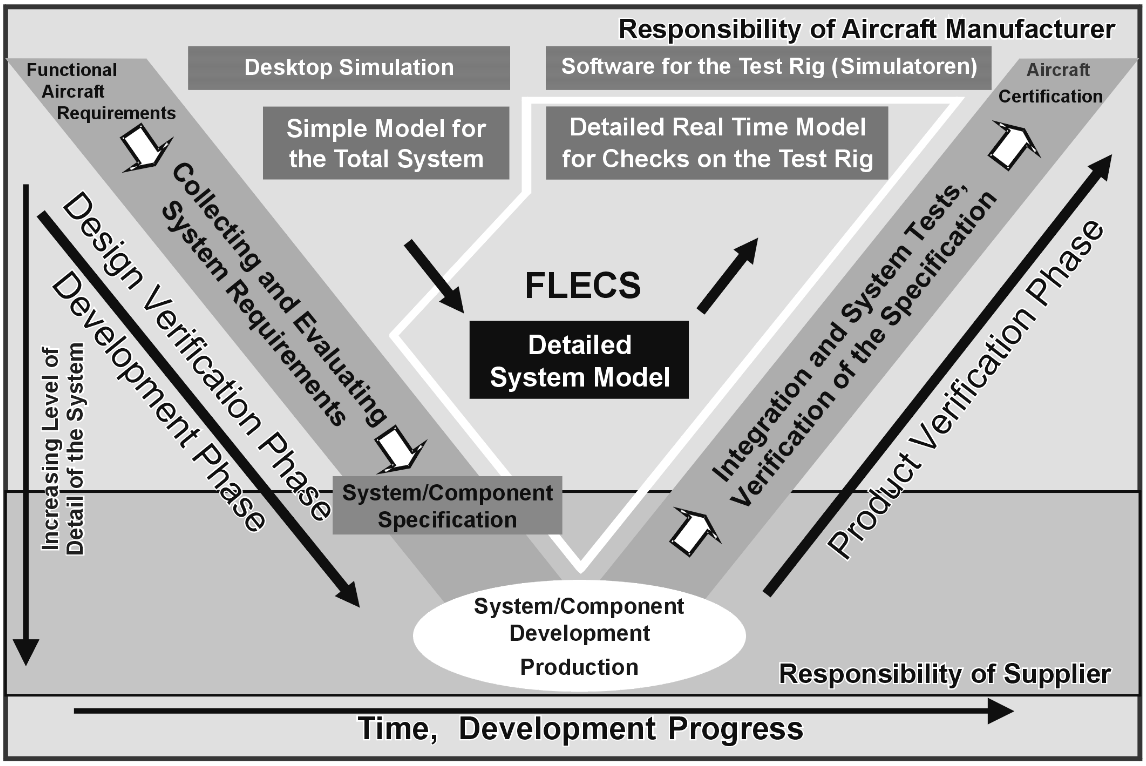

Figure 1: Simulation in the system development process of an aircraft manufacturer

During the specification process an iterative process of Design Verification is carried out, to check if the more and more detailed design fulfills the requirements of the different specification levels. Right after first software and hardware prototypes have been developed, the iterative Product Verification processes start. This is to verify, if the now available products comply with the requirements they have been developed to. Usually information and responsibility for a certain task is handed over to another person, department or company.

Nevertheless, the final product is integrated into an aircraft, for which the aircraft manufacturer is held responsible.

Component classes: Each component of the Environmental Control System has to be mapped by a MATLAB/Simulink model block. Several component classes were defined for FLECS:

- Ambient conditions
- Aircraft boundaries
- Flow resistances
- Flow and pressure sources
- Volumes
- Area models
- Mixing unit
- Heat exchangers
- Air cycle machine and air compressor
- Ram flow
- Vapor cycle systems
- Sensors
- Controls

Each FLECS component class contains a number of models for each aircraft components considered. The real world behavior has to be reproduced by a physical description using the appropriate functions. To assure high flexibility and a large application range, modeling has to be as general as possible. This leads to three different model types "Detailed Dynamic". Simplifications of the models introduced in a second step, lead to the types "Simple Dynamic" and "Pre-Design" that enhance stability of the simulation and reduce simulation time.

Static design of the ECS: The environmental control system can be designed statically from top level aircraft requirements like number of passengers, mission range of the aircraft, operational envelope, maximum cabin altitude etc., if additionally the different heat loads and heat capacities inside the cabin are known or estimated. Results from a static ECS design are for example the necessary pack and recirculation mass flow.

Dynamical design of the ECS: Based on parameters from the static ECS design, a dynamical simulation can be built up. The design of an ECS has to ensure, that different time dependent scenarios, like the pull down case (cooling) or pull up case (heating) are fulfilled. With a simulation it can be assured that dynamic requirements are met. A simulation can furthermore be used to determine the parameters of the various controllers in the system, as there are the pack controllers or the cabin & duct controller.

Aircraft cabin temperature control and ventilation: The principal configuration of an ECS is shown in Figure 2. A cabin is divided into cabin zones. The temperature in each zone is controlled by an independent trim air valve. Conditioned air from the air generation packs and re-circulated air from the cabin are mixed inside the mixing unit. From the mixing unit the air flows to the mixing point, where a small amount of hot trim air is added to achieve the selected cabin temperature.

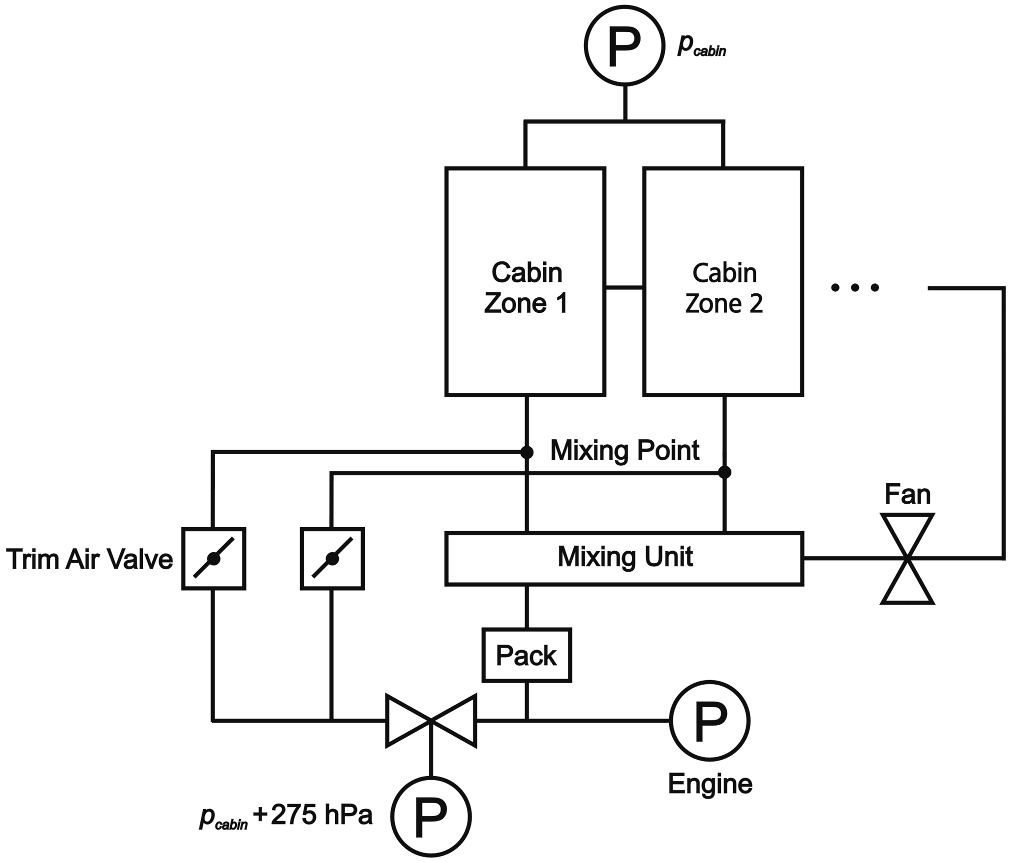

Figure 2: Schematic drawing of the environmental control system

The cabin zone with the lowest target temperature defines the required temperature inside the mixing unit. The trim air valve of this cabin zone is (almost) closed. The opening angles of the trim air valves of the other zones are opened that much as to allow enough hot air to pass into the respective duct to the cabin to achieve the demanded cabin zone air temperature. For an ECS two independent controller types are used to ensure all this: The pack controller controls the pack and hence the pack air temperature. The cabin & duct controller controls primarily the opening angle of the trim air valve and hence the cabin zone temperature. Details of control algorithms of existing aircraft are proprietary data of the respective equipment supplier.

Temperature control details follow from Figure 3. The cabin and duct controller is a serial connection of a PI-type cabin controller, which defines the target temperature for the duct controller. The controlled variable of the cabin & duct controller is the supply temperature in the mixing point. The actuating variable of the duct controller is angular velocity of the opening angle of the trim air valve. The temperature of the pack is controlled by the pack controller.

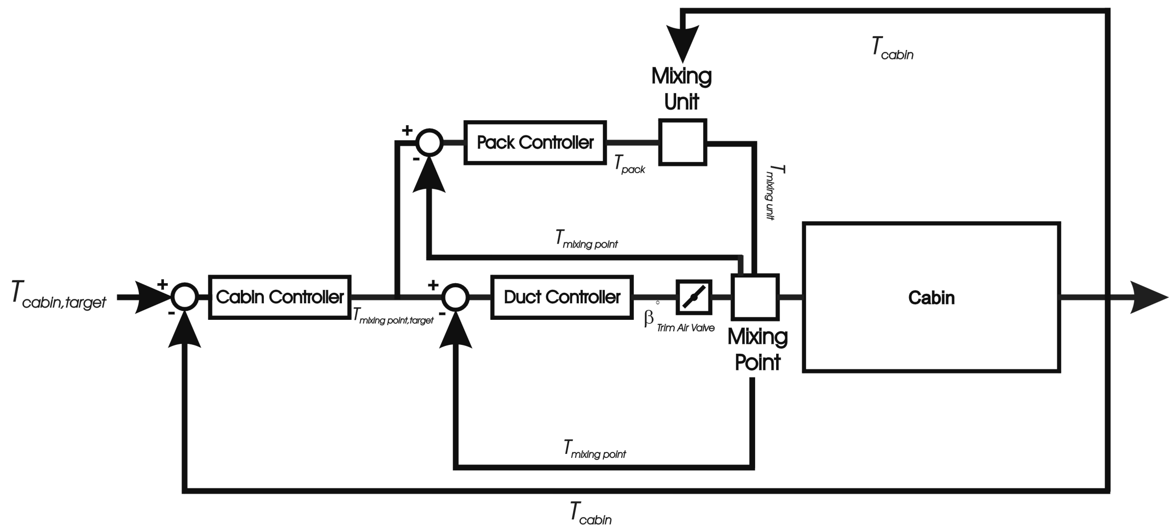

Figure 3: The control aspects of a cabin simulation

As goal of the project each system component should be related to a specific model block. The description of the accurate parameterization of the physical processes within a model-block is a major task of this Technical Note (TN: *Technical Note*).

The dynamical behavior of the system is described by state variables, in the following also called dynamical input and output variable. For every dynamical variable a time dependant state equation has to be solved. The thermodynamic and mathematic characterization of these equations should ensure a stable and a real-time capable algorithm. The fundamental configuration respectively the parameterization of this system will be discussed on the basis of a network of volume elements and duct elements. The physical behavior of this basis system is well known, therefore the control of the right mode of operation is ensured.

2 Basic Consideration

With Help of the database elements system simulation can be generated, within these configurations the response to time dependant boundary conditions, and second the system response to certain failure cases can be investigated. These requirements demand a software interface, which enables time resolved simulations. In industry and scientific research institutes, MATLAB/Simulink is a widespread software platform. MATLAB/Simulink provides high degree of functionality and flexibility. The features allow building up a user-friendly database, which can be adapted to the given specifications.

The inner structure of MATLAB/Simulink is combined with the characterization of time-dependant systems. For each time-step *dt* within a given time-range *Δt* the states of the simulated system are calculated. The state of the system is specified by a set of state variables. The set of state variables is related to a set of state equations (see Figure 4).

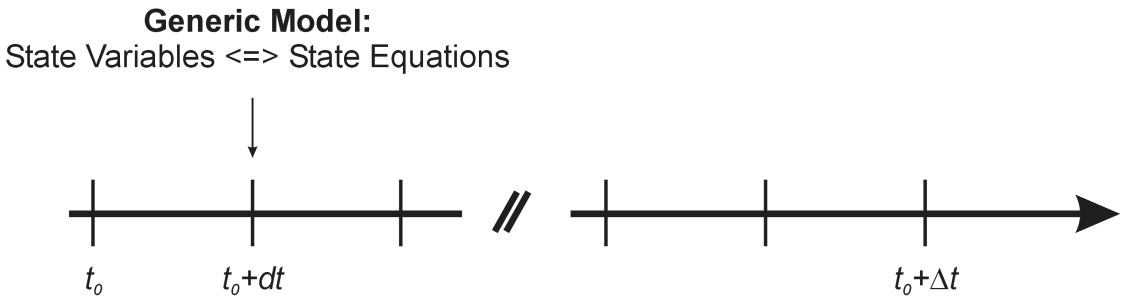

Figure 4: The inner structure of an MATLAB/Simulink system

Two types of state equations can be distinguished. At first time-dependant rates equations (see Equation 1).

$$\frac{dy(t)}{dt} = f(y(t);t) \tag{1}$$

In general $f(y(t);t)$ is not only function of $y(t)$, but also a function of other time-dependant variables. Equations according to form Equation 1 are solved by an integrator (see Equation 2).

$$y_i = \sum_{j=1}^{i-1} dy_j + \underbrace{\left[\int_{t_0+(i-1)\,dt}^{t_0+i\,dt} f(y_{(i-1)}(t);t)\,dt \right]}_{dy_i} + y_{init}\ , i = 1 \ldots N,\ \Delta t = N\,dt,\ dy_0 = 0 \tag{2}$$

Equation 2 is only solvable, if the initial parameters for each state variable are known. The second type of state equations is a quasi stationary equation (see Equation 3).

$$y(t) = f(t) \tag{3}$$

These Equations are solvable without any knowledge of initial parameters. The third type of equations is the steady state type (see Equation 4).

$$y(t) = y = Const \tag{4}$$

The integrator in Equation 2 is an intrinsic function block of MATLAB/Simulink. The functionality of the integrator is associated to the chosen solver mode. The solver function defines the step size dt and the algorithm of integration. MATLAB/Simulink makes available two different solver species. A fixed step solver and a variable step solver. For the developed model-blocks it should be ensured, that both Solver type are usable, because different processes with different time velocity constants are looked at.

3 Nomenclature of Physical Values

The model blocks can be characterized with two different groups of values. The first group includes the constants and the parameters. By the constants the medium inside the system is defined. In Addition the Parameters characterizes the component itself. For example a flow resistance can be parameterized by a diameter D and a length L. The second group includes the state variables. The related state equations are based on thermo dynamical and mechanical considerations. The time dependant state equations are only solvable, if the initial parameters are known.

In Figure 5 the configuration of a model block is shown in principle. A block receives a set of dynamical inputs from one or more other components. Using the initial parameters, a set of dynamical outputs can be calculated. This set is transferred to the neighboring components.

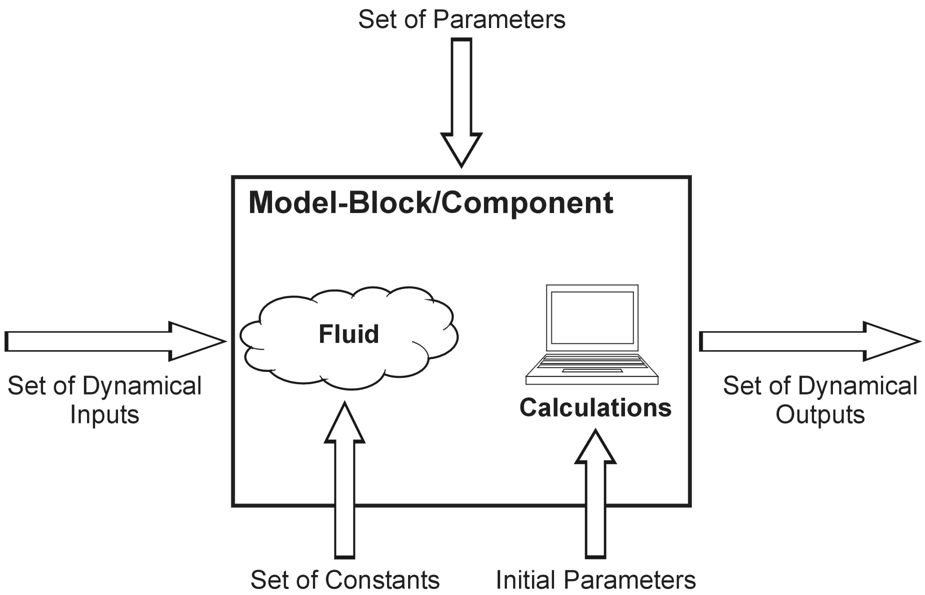

Figure 5: The principal configuration of a model block

In Table 1 the constants, parameters and state variables of a generalized volume, respectively its initial parameters are combined. Each value is connected with a specific symbol, a label and a unit. In this TN the units are always given in International System of Units (SI). The Symbols are given by literature and standards. Inside the Model-blocks for each value a characteristic label name is used. By the following rules the symbols are translated into the labels. The transfer of subscripts and superscripts is shown by the following example.

$$p_{init} \Leftrightarrow p\_init$$

Greek symbols are transposed in Latin letters.

$$\eta \Leftrightarrow eta$$

Table 1: List of constants, parameters, state variables and initial parameters of a generalized volume

Constants	Symbol	Label Name	Unit
Intrinsic Gas Constant			
Dry Air	R_{air}	R_air	J/kg K
Water Vapor	$R_{H2O,gas}$	R_H2O_gas	J/kg K
CO_2	R_{CO2}	R_CO2	J/kg K
Specific Heat Capacity			
Dry Air	$c_{p,air}$, $c_{v,air}$	c_p_air, c_v_air	J/kg K
Water Vapor	$c_{p,H2O,gas}$, $c_{v,H2O,gas}$	c_p_ H2O_gas, c_v_ H2O_gas	J/kg K
CO_2	$c_{p,CO2}$, $c_{v,CO2}$	c_p_ CO2, c_v_ CO2	J/kg K

Parameters	Symbol	Label Name	Unit
Volume	V	V	m^3

State Variables	Symbol	Label Name	Unit
Pressure	p	p	Pa
Temperature	T	T	K
Mass Dry Air	m_{air}	m_air	kg
Mass Water Vapor	$m_{H2O,gas}$	m_H2O_gas	kg
Mass CO_2	m_{CO2}	m_CO2	kg
Mass Free Water	$m_{H2O,liq}$	m_H2O_liq	kg

Initial Parameter	Symbol	Label Name	Unit
Pressure	p_{init}	p_init	Pa
Temperature	T_{init}	T_init	K
Mass Water Vapor	$x_{H2O,gas,init}$	x_H2O_gas_init	kg/kg
Mass CO_2	$x_{CO2,init}$	x_CO2_init	kg/kg
Mass Free Water	$x_{H2O,liq,init}$	x_H2O_gas_init	kg/kg

The gas mixture inside the system is characterized by an average intrinsic gas constant $\overline{R}$. In dry air flow system the intrinsic gas constant has the value $R = 287.058$ J/kg K. Under assumption of ideal gas condition the specific heat capacities has the values $c_p = 7/2\ R$ and $c_v = 5/2\ R$. Between R, c_p and c_v exists the relationship (see Equation 5).

$$R = c_p - c_v \tag{5}$$

Each block of the FLECS database can be parameterized by a specific input mask.

4 Topology

The in this TN simulations of airflow systems are discussed, which shows a topology described in Figure 6. The networks consist of sinks, flow resistances, volumes, nodes, heat resistances and sources.

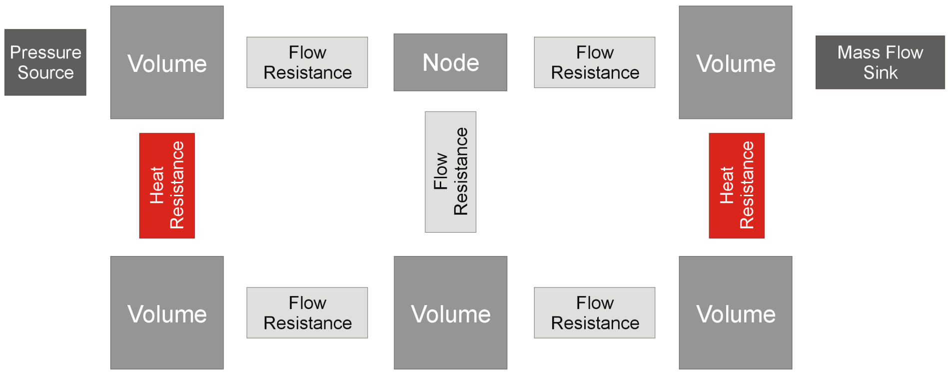

Figure 6: An example of a topology of an airflow simulation

With the help of the shown structure systems with a different degree of complexity could be built up. In addition the physical behavior of such systems is well known. Therefore airflow networks could be used as test system.

A fundamental difference between real components and MATLAB/Simulink blocks is thereby given, that one physical aperture is related to one input and one output (see Figure 7).

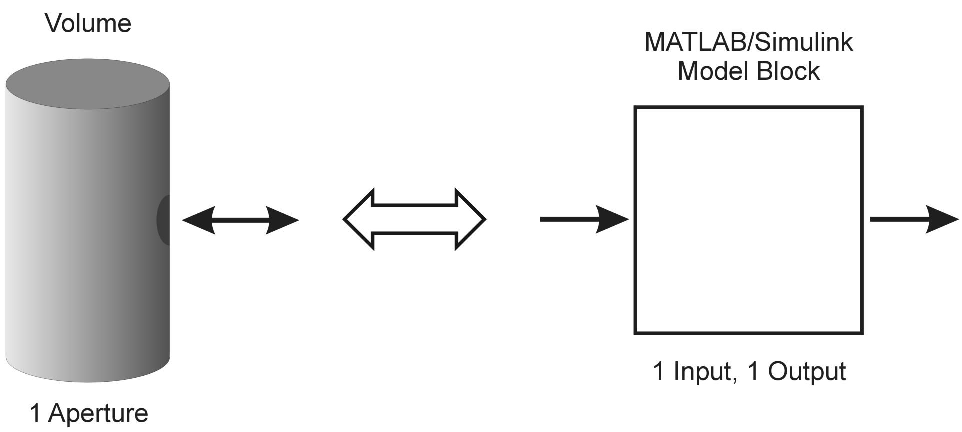

Figure 7: The transition from a real ECS-component to MATLAB/Simulink model block

In this connection is the arrow direction (see Figure 4) isn't linked to the direction of the air flow. Each component transfers its information about the state variables to his neighbors (see Figure 8), otherwise the neighboring blocks transfer back their information. This configuration of a modular MATLAB/Simulink simulation model is called a feedback structure.

The ambient conditions of the simulation are given by end pieces like Sinks and Sources. The class of volume components spans the model blocks of generalized, an specialized volumes and nodes, and the class of flow components enfolds the models of a incompressible and compressible flow resistance (FR: *Flow Resistance*) .

The number of apertures defines the dimensionality of the volumes. The notation Vol_1D indicates, that the simulated volume has one aperture, respectively the model-block has one input and one output. A volume element is defined by the state variables pressure, density and temperature. Therefore in the case of volumes the dimensionality of the outputs is limited to one (see Figure 8).

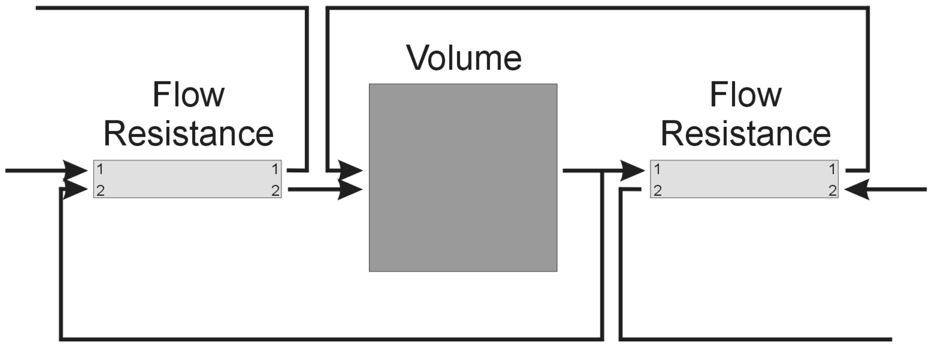

Figure 8: Feedback structure of a MATLAB/Simulink model (duct model, see also Section 5.4)

5 Physical Properties and the Description of the Algorithm

In this section the inner structure of the algorithm is derived by thermodynamic considerations. The performance of a component is described by state variables and state equations. The dynamical behavior of a set variable can be specified by a set of rate equations. The derivation of this rate equation bases of energy balance considerations. The state variables are shown in Table 1. In general the set of the pressure p, the density ρ and the temperature T are the dynamical variables of components with intrinsic volume. The different specifications of the different block types can be found in the TN FLECS_WP2_TN_SRD-Release of Airbus. In this TN physical models have been developed, which fulfill this specifications.

5.1 Volume Properties

The first fundamental theorem of thermodynamics presents the relationships between the enthalpy H and the intrinsic energy U and the work $p\ V$ (see Equation 6).

$$H(t) = U(t) + p(t)\,V \tag{6}$$

As a first approximation the difference of the potential energy and the kinetic energy of the start and end state of a system is neglected. In this case Equation 6 can be written in a differential form shown in Equation 7.

$$\frac{dH(t)}{dt} = (\dot{Q}(t) + \Delta\dot{H}(t)) + V(t)\frac{dp(t)}{dt} + \underbrace{[p(t)\frac{dV(t)}{dt}]}_{0} \tag{7}$$

In general the volume is a permanent parameter of the system *($V(t)$ = Const, isochore)*. Under this assumption the term within the square brackets in Equation 7 can be neglected. With Equation 7 also systems can be treated, which are heated up or cooled down by an external heat source with a heat transfer rate $\dot{Q}$. The different types of heat transfer processes will be discussed in an own section. $\Delta\dot{H}$ specifies the enthalpy flow, which enters into the system, respectively leaves the system.

The enthalpy H is the product by the specific enthalpy h and the mass $m = \rho\ V$ of the system (see Equation 8).

$$H(t) = m(t)\ h(t) \tag{8}$$

The differential form of Equation 8 (see Equation 9) can be inserted in Equation 7. The result is shown in Equation 10.

$$\frac{dH(t)}{dt} = V\,\rho\,(t)\,\frac{dh(t)}{dt} + V\,h(t)\,\frac{d\rho\,(t)}{dt} \tag{9}$$

$$\rho\,(t)\,\frac{dh(t)}{dt} + h(t)\,\frac{d\rho\,(t)}{dt} = \frac{1}{V}\,(Q_{dot}(t) + W_{dot}(t) + \Delta\dot{H}(t)) + \frac{dp(t)}{dt} \tag{10}$$

dh/dt and h in Equation 10 have the form (see Equation 11).

$$\begin{aligned} h(t) &= c_p\,T(t) \\ \frac{dh(t)}{dt} &= c_p\,\frac{dT(t)}{dt} \end{aligned} \tag{11}$$

Under assumption of ideal gas condition the operator dp/dt in Equation 10 can be replaced by Equation 12.

$$\begin{aligned} p(t) &= R\,\rho\,(t)\,T(t) \\ \Rightarrow\ \frac{dp(t)}{dt} &= R\,\rho\,(t)\,\frac{dT(t)}{dt} + R\,T(t)\,\frac{d\rho\,(t)}{dt} \end{aligned} \tag{12}$$

The end result of these considerations is a state equation for the temperature T (see Equation 13)

$$\frac{dT(t)}{dt} = \frac{1}{V\,\rho\,(t)\,c_v}\,(\dot{Q}(t) + \Delta\dot{H}(t)) - \frac{T(t)}{\rho\,(t)}\,\frac{d\rho\,(t)}{dt} \tag{13}$$

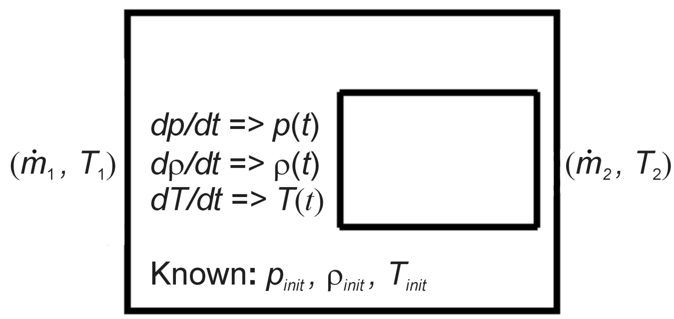

Figure 9: Inner structure of a volume

Under the assumption, that a gas flow described by a mass flow $\dot{m}_{in} = \dot{m}_1 > 0$, a temperature T_{in} and a specific heat capacity $c_{p,in}$ enters the system and a gas flow described by a mass flow $\dot{m}_{out} = |\dot{m}_2|, \dot{m}_2 < 0$ leaves (see Figure 9) the system, the differential enthalpy flow $\Delta\dot{H}$ can be written according Equation 14. The temperature T_{out} and the specific heat capacity $c_{p,out}$ of the outgoing flow are defined by the gas mixture inside the volume ($T_{out} = T$, $c_{p,out} = c_p$).

$$\Delta \dot{H}(t) = \dot{m}_{in}(t)\, c_{p,in}\, T_{in}(t) - \dot{m}_{out}(t)\, c_p\, T(t) \tag{14}$$

The state equation of the density ρ arises out of the mass balance of the system (see Equation 15).

$$\frac{d\rho\,(t)}{dt} = \frac{1}{V}\frac{dm(t)}{dt} = \frac{\dot{m}_{in}(t) - \dot{m}_{out}(t)}{V} \tag{15}$$

With help of Equation 13 and Equation 15 the rate equation of the pressure p can be calculated using Equation 12. Under the assumption, that the gas obeys the ideal gas conditions, only two of three state variables are independent. By a given mass flow $\dot{m}$ the system is defined over of the pressure p, the density ρ and the temperature T.

The equations Equation 12, Equation 13 and Equation 15 can be adapted to different special cases.

1. Isobar: $p = Const,\ dp/d\,t = 0$
2. Adiabatic: $\dot{Q} = 0$

5.1.1 The Kinetic Energy

In an airflow system a certain mass per time step is pushed around. In such system the kinetic energy normally has to be considered. The volume described above works in static mode. The calculated pressure, temperature and density are static. As long as the simulations are limited to systems, there the average flow velocities v are in the order of few kg/s, a differentiation between total pressure p_{total} and static pressure p_{static} are not implicitly essential. The relation between the static pressure and the total pressure is defined by equation Equation 16.

$$p_{total} = p_{static} + \frac{1}{2}\rho\ v^2 \tag{16}$$

For example, in the case, that the flow velocity is 1 m/s, the static pressure is equal 101300 Pa and the density is 1.203 kg/m³, then the total pressure differs less then 1%.

5.2 Generalized Volume with Water Vapor, CO_2 and Free Water Balance

Table 2: Input and output variables of a volume with water vapor, CO_2 and free water balance

Input Variables	Output Variables
Temperature	Pressure
Mass Flow Dry Air	Density
Water Vapor Content	Temperature
CO_2 Content	Mass Dry Air
Water Content	Water Vapor Content
	CO_2 Content
	Water Content

In general the air flow is characterized by a certain number N of mass flows $\dot{m}_i$, $i = 1 \ldots N$. Each air flow requires a one input. If $\dot{m}$ is positive, the mass flows into the component, respectively if $\dot{m}$ is negative, the air leaves the component. The gas mixture of the considered air flow systems consists of a gas mixture composed of dry air, water vapor and CO_2 (see Table 2). The specific constants of these different gases are (see Table 3):

Table 3: Specific constants of the gas mixture

R_{air}	=	287.058	J/kg K
$R_{H2O,gas}$	=	461.523	J/kg K
R_{CO2}	=	188.924	J/kg K
$c_{p,air}$	=	1005	J/kg K
$c_{p,H2O,gas}$	=	1870	J/kg K
$c_{p,CO2}$	=	830	J/kg K

The values for c_v can be calculated with Equation 5. All these values are valid under standard conditions. The free water inside the system is characterized by the specific heat capacity $c_{H2O,liq}$ (see Table 4).

Table 4: Specific constants of the free water

$c_{H2O,liq}$	=	4173 J/kg K, $T \geq 273.15$ K
		2050 J/kg K, $T < 273.15$ K

In the case of a gas mixture composed of pure air, water vapor (H2O,gas) and CO_2 the total enthalpy H of a system can be written as (see Equation 17):

$$H(t) = m_{air}(t)\, c_{p,air}\, T(t) + m_{H2O,gas}(t)\, c_{p,H2O,gas}\, T(t) + m_{CO2}(t)\, c_{p,CO2}\, T(t) \tag{17}$$

The total pressure accords to Equation 18.

$$p(t) = \underbrace{R_{air}\, \frac{m_{air}(t)}{V}\, T(t)}_{p_{air}} + \underbrace{R_{H2O,gas}\, \frac{m_{H2O,gas}(t)}{V}\, T(t)}_{p_{H2O,gas}} + \underbrace{R_{CO2}\, \frac{m_{CO2}(t)}{V}\, T(t)}_{p_{CO2}} \tag{18}$$

The mass balance of the system has to be divided in a mass balance for the total mass m and for the partial masses m_{air}, $m_{H2O,gas}$, m_{CO2} (see Equation 19).

$$\begin{gathered}
\frac{dm(t)}{dt} = \dot{m}_{air,in}(t) - \dot{m}_{air,out}(t) + \dot{m}_{H2O,gas,in}(t) - \dot{m}_{H2O,gas,out}(t) + \dot{m}_{CO2,in}(t) - \dot{m}_{CO2,out}(t) \\
\frac{dm_{air}(t)}{dt} = \dot{m}_{air,in}(t) - \dot{m}_{air,out}(t) \\
\frac{dm_{H2O,gas}(t)}{dt} = \dot{m}_{H2O,gas,in}(t) - \dot{m}_{H2O,gas,out}(t) \\
\frac{dm_{CO2}(t)}{dt} = \dot{m}_{CO2,in}(t) - \dot{m}_{CO2,out}(t)
\end{gathered} \tag{19}$$

The state equation of the temperature (see Equation 20) can be derived from using Equation 17 … 19 and Equation 7.

$$\begin{gathered}
\frac{dT(t)}{dt} = \\
[\dot{Q} + \dot{m}_{air,in}(t)\,(c_{p,air}\, T_{in}(t) - c_{v,air}\, T(t)) - \dot{m}_{air,out}(t)\,(c_{p,air}\, T(t) - c_{v,air}\, T(t)) \\
+ \dot{m}_{H2O,gas,in}(t)\,(c_{p,H2O,gas}\, T_{in}(t) - c_{v,H2O,gas}\, T(t)) - \dot{m}_{H2O,gas,out}(t)\,(c_{p,H2O,gas}\, T(t) - c_{v,H2O,gas}\, T(t)) \\
+ \dot{m}_{CO2,in}(t)\,(c_{p,CO2}\, T_{in} t) - c_{v,CO2}\, T(t)) - \dot{m}_{CO2,out}(t)\,(c_{p,CO2} \cdot T(t) - c_{v,CO2}\, T(t))]/ \\
[\frac{1}{m_{air}(t)\, c_{v,air} \cdot + m_{H2O,gas}(t)\, c_{v,H2O,gas} + m_{CO2}(t)\, c_{v,CO2}}]
\end{gathered} \tag{20}$$

In gas mixtures the specific constants R, c_p and c_v exchange into time dependant average values $\overline{R}(t)$, $\overline{c}_p(t)$ and $\overline{c}_v(t)$ (see Equation 21).

$$\bar{R}(t) = \frac{m_{air}(t)\, R_{air} + m_{H2O,gas}(t)\, R_{H2O,gas} + m_{CO2}(t)\, R_{CO2}}{m_{air}(t) + m_{H2O,gas}(t) + m_{CO2}(t)}$$
$$\bar{c}_p(t) = \frac{m_{air}(t)\, c_{p,air} + m_{H2O,gas}(t)\, c_{p,H2O,gas} + m_{CO2}(t)\, c_{p,CO2}}{m_{air}(t) + m_{H2O,gas}(t) + m_{CO2}(t)} \tag{21}$$
$$\bar{c}_v(t) = \frac{m_{air}(t)\, c_{v,air} + m_{H2O,gas}(t)\, c_{v,H2O,gas} + m_{CO2}(t)\, c_{v,CO2}}{m_{air}(t) + m_{H2O,gas}(t) + m_{CO2}(t)}$$

The equations Equation 19 … 20 and the Equation 12 are characteristic for each component with an intrinsic volume.

Within an airflow related to a certain amount of humidity the condensation and evaporation of water plays an important role. In a certain air volume V_{air} at the temperature T only a maximum mass of water vapor can be stored (see Figure 10). This saturation density $\rho_{H2O,gas,sat}$ of water vapor is only a function of the temperature ($\rho_{H2O,gas,sat} = \rho_{H2O,gas,sat}(T)$) and is independent on the total pressure p of the gas mixture. Normally the air flow systems are driven in a temperature range of -50 °C … 200 °C and in a pressure range of 10^5 Pa …10^6 Pa.

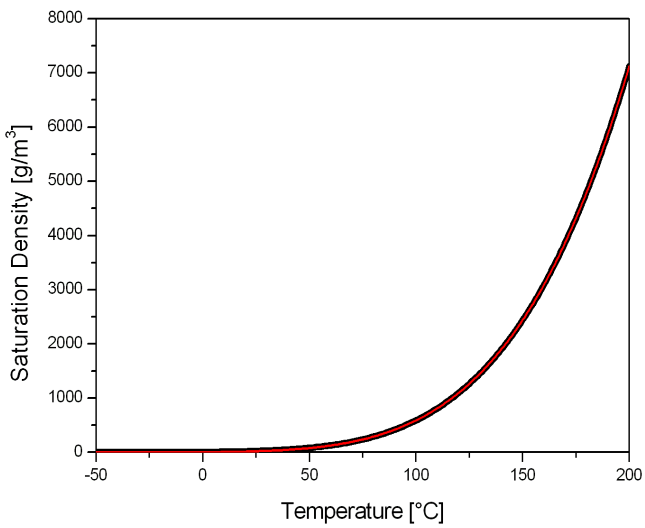

Figure 10: The saturation density of water vapor in air, as function of the temperature. Black line: measured data, red line: fit function (see text)

The black line in Figure 8 shows the measured saturation density $\rho_{H2O,gas,sat}$, which can be found in literature. The red line shows a fit function $\rho_{H2O,gas,sat,fit}(T)$ (see Equation 22) of the measured data.

$$\rho_{H2O,gas,sat,fit}(T) = K_0 \exp(K_1\, (T - 273.15\text{ K})/(K_2 + (T - 273.15\text{ K}))) \tag{22}$$

With the parameter-set $K_0 = 4.44259$ g/m^3, $K_1 = 15.05703$ and $K_2 = 208.07254$ K. The fit function $\rho_{H2O,gas,sat,fit}(T)$ is in good agree with the saturation density $\rho_{H2O,gas,sat}(T)$. By a given temperature T, $\rho_{H2O,gas,sat}$ is related to the saturation pressure $p_{H2O,gas,sat}(T)$ (s ee Figure 9). $p_{H2O,gas,sat}(T)$ can be fitted by the same function type as $\rho_{H2O,gas,sat,fit}(T)$ (see Equation 22) using the parameter set $K_0 = 595.14519$ Pa, $K_1 = 16.78355$ and $K_2 = 226.6284$ K.

Within the simulation the moisture content $x_{H2O,gas}$ respectively the CO_2 content x_{CO2} are treated as dynamical outputs. The moisture content is the relation between the mass of the water vapor $m_{H2O,gas}$ and the mass of the air m_{air}, and can be expressed by the mole mass M_{H2O} and M_{air} of water and air ($M_{H2O} = 18.02$ g/mol, $M_{air} = 28.96$ g/mol) the total pressure and the partial pressure of water and CO_2 (see Equation 23) .

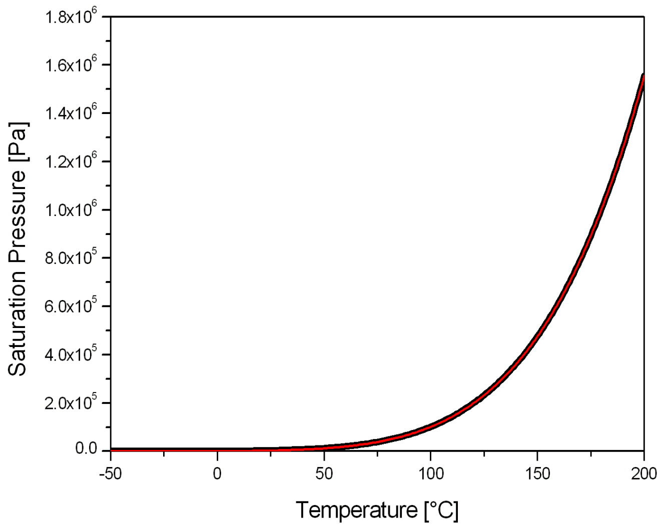

Figure 11: The saturation pressure of water vapor in air, as function of the temperature. Black line: measured data, red line: fit function (see text)

$$x_{H2O,gas}(t) = \frac{m_{H2O,gas}(t)}{m_{air}(t)} = \frac{M_{H2O}}{M_{air}} \frac{p_{H2O,gas}(t)}{p(t) - p_{H2O,gas}(t) - p_{CO2}(t)} \tag{23}$$

Analogous to this definition then CO2-content x_{CO2} can be defined ($M_{CO2} = 44.01$ g/mol) (see Equation 24).

$$x_{CO2}(t) = \frac{m_{CO2}(t)}{m_{air}(t)} = \frac{M_{CO2}}{M_{air}} \frac{p_{CO2}(t)}{p(t) - p_{H2O,gas}(t) - p_{CO2}(t)} \tag{24}$$

In addition to $x_{H2O,gas}$ and x_{CO2} also the mass of the free water inside the system is standardized on the mass of air (see Equation 25).

$$x_{H2O,liq}(t) = \frac{m_{H2O,liq}(t)}{m_{air}(t)} \tag{25}$$

In the saturation case $p_{H2O,gas}(t)$ has to be replaced by $p_{H2O,gas,sat}(T)$ (see Figure 11) . The humidity φ of an air mixture is defined by the relation between the density of the water vapor $\rho_{H2O,gas}(t)$ and the saturation density $\rho_{H2O,gas,sat}(T)$ (see Equation 26) .

$$\varphi = 100\% \cdot \frac{\rho_{H2O,gas}(t)}{\rho_{H2O,gas,sat}(T)} \tag{26}$$

The inner structure of a generalized volume with water vapor, CO_2 and free water balance is shown in Figure 12.

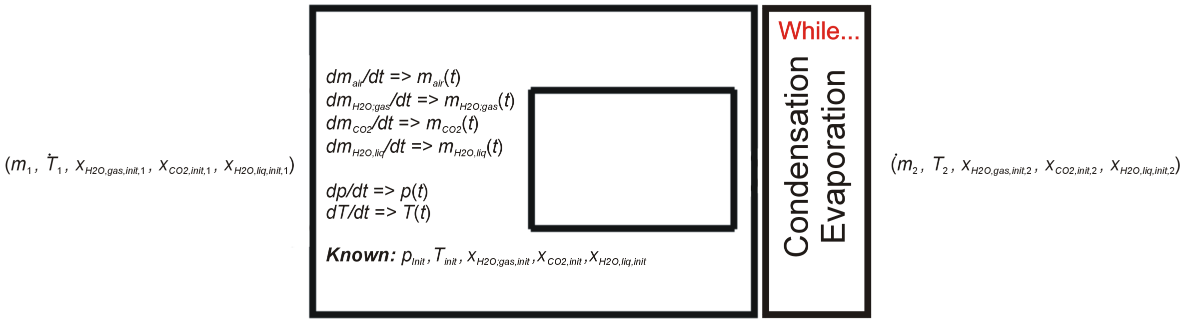

Figure 12: Inner structure of a generalized volume with water vapor, CO_2 and free water balance

5.3 Condensation and Evaporation

Table 5: Input and output variables of a condensation/evaporation block

Input Variables	Output Variables
Temperature	Temperature
Mass Dry Air	Mass Dry Air
Water Vapor Content	Water Vapor Content
CO_2 Content	CO_2 Content
Water Content	Water Content

If the humidity overshoots 100% condensation occurs, on the other hand if the humidity is less then 100% and within the system free water is found, evaporation takes place. In the case of condensation the gas has a gain of condensation heat Δh_{cond}, in the case of evaporation there is a loss of evaporative cooling Δh_{evap} inside the water. The specific enthalpies of condensation Δh_{cond} and evaporation Δh_{evap} have the same value (see Figure 13) and are only functions of the temperature. Inside a wet gas an amount of latent heat is stored. During the phase change gas – liquid (condensation) this energy $\Delta h_{cond} = m_{cond}\, r_{0,cond}$ (m_{cond}: mass of condensed water) is given free, therefore the temperature of the gas in closed adiabatic system rises up. On the other hand during the phase change liquid – gas (evaporation) the free water has to enrage the energy $\Delta h_{evap} = m_{evap}\, r_{0,evap}$ (m_{evap}: mass of evaporated water) and the temperature in closed adiabatic system are reduced. In the following consideration an average specific enthalpy $r_{0,cond} = r_{0,evap} = r_0 = 2500000$ J/kg is assumed.

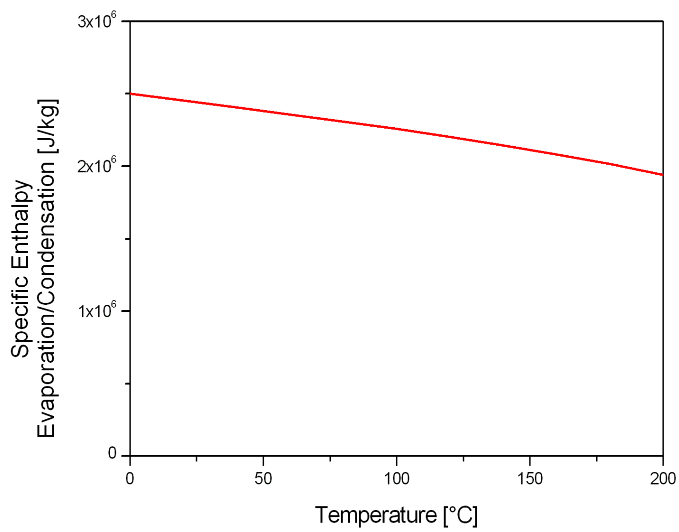

Figure 13: The enthalpy of evaporation and condensation as function of the temperature

Basic Assumption

In the following considerations are at the bottom of the assumption, that the processes of condensation and evaporation take place instantaneously. Therefore the different thermodynamic processes can be treated independently. For example then two gas amounts with different temperatures and different moisture contents mixed together, at first the mixing process is treated and afterwards the condensation/evaporation process is evaluated.

In general the model described has to be distinguished between temperature of the gas mixture T and the temperature of the free water $T_{H2O,liq}$. In the following considerations the free water in the system is assumed to be is in the thermal equilibrium with the ambient gas, the temperature $T_{H2O,liq}$ becomes equal to the temperature T. Therefore the state equations for the free water can be neglected.

Assuming that the condensation process ($m_{H2O,gas} > m_{H2O,gas,sat}(T)$) takes place instantaneously in good approximation the following enthalpy equation has to be solved (see Equation 27).

$$\begin{aligned}&\underbrace{(m_{air}\ c_{p,air}+m_{H2O,gas}\ c_{p,H2O,gas}+m_{CO2}\ c_{p,CO2})\,T}_{1}+\underbrace{m_{H2O,liq}\ c_{H2O,liq}\ T}_{2}=\\&\underbrace{(m_{air}\ c_{p,air}+m_{H2O,gas,sat}(T')\,c_{p,H2O,gas}+m_{CO2}\ c_{p,CO2})\,T'}_{3}-\underbrace{(m_{H2O,gas}-m_{H2O,gas,sat}(T'))\,r_0}_{4}\\&\underbrace{(m_{H2O,liq}+m_{H2O,gas}-m_{H2O,gas,sat}(T'))\,c_{H2O,liq}\ T'}_{5}+\underbrace{(m_{H2O,gas}-m_{H2O,gas,sat}(T'))\,r_{ice}(T)}_{6}\end{aligned} \qquad (27)$$

The expression 1 in Equation 27 is the enthalpy of the gas after mixing. Expression 2 is the enthalpy of the liquid or frozen water inside the system before condensation. For liquid water (T > 273.15 K) the specific heat capacity is $c_{H2O,liq}$ = 4173 J/kg K. In the case of frozen water the specific heat capacity is $c_{H2O,liq}$ = 2050 J/kg K. The expression 3 is the enthalpy of the gas after condensation. The temperature of the gas mixture has risen up to T'. The expression 4 is the gain of condensation heat. The expression 5 is the enthalpy of the liquid or frozen water inside the system after condensation. The expression 6 describes the gain of heat of fusion. The specific enthalpy of fusion $r_{ice}(T)$ is 0 for $T \geq$ 273.15 K and 333000 J/kg for $T <$ 273.15 K. Equation 27 can't be solved analytically, only a numerical solution for a given parameter set (m_{air}, $m_{H2O,gas}$, m_{CO2}, $m_{H2O,liq}$, T) can be calculated.

The process of Evaporation takes place in a system consisting of a gas mixture with humidity less then 100% and a certain amount of water $m_{H2O,liq}$. Before evaporation the gas has the temperature T and a mass $m_{H2O,gas}$ of water vapor stored. The mass $m_{H2O,gas}$ is smaller then the saturation mass $m_{H2O,gas,sat}(T)$ ($m_{H2O,gas,sat}(T) < m_{H2O,gas}$). In this case the water is evaporated, until the saturation mass of water vapour ($m_{H2O,gas}' = m_{H2O,gas}+\Delta m = m_{H2O,gas,sat}(T')$) is reached or the total amount of water is exhausted ($m_{H2O,gas}' = m_{H2O,gas}+ m_{H2O,liq} \leq m_{H2O,gas,sat}(T')$). Based on this situation the following enthalpy equation can be developed (see Equation 28).

$$\begin{aligned}
&\underbrace{(m_{air}\ c_{p,air} + m_{H2O,gas}\ c_{p,H2O,gas} + m_{CO2}\ c_{p,CO2})\ T}_{1} + \underbrace{m_{H2O,liq}\ c_{H2O,liq}\ T}_{2} = \\
&\underbrace{(m_{air}\ c_{p,air} + m_{H2O,gas}{}'\ c_{p,H2O,gas} + m_{CO2}\ c_{p,CO2})\ T'}_{3} + \underbrace{(m_{H2O,gas}{}' - m_{H2O,gas})\ r_0}_{4} \\
&\underbrace{(m_{H2O} - m_{H2O,gas}{}' + m_{H2O,gas})\ c_{H2O,liq}\ T_{H2O}}_{5} - \underbrace{(m_{H2O,gas}{}' - m_{H2O,gas})\ r_{ice}(T)}_{6}
\end{aligned} \qquad (28)$$

Equation 27 and 28 can be transformed in a more general way by dividing the equations by the mass of the dry air. In this case the enthalpy equations are transferred into equations of the specific enthalpy *h* of the system. For the condensation process this transformation is shown in Equation 29.

$$\begin{aligned}
&(c_{p,air} + x_{H2O,gas}\ c_{p,H2O,gas} + x_{CO2}\ c_{p,CO2})\ T + x_{H2O,liq}\ c_{H2O,liq}\ T = \\
&(c_{p,air} + x_{H2O,gas,sat}(T')\ c_{p,H2O,gas} + x_{CO2}\ c_{p,CO2})\ T' - (x_{H2O,gas} - x_{H2O,gas,sat}(T'))\ r_0 \\
&(x_{H2O,liq} + x_{H2O,gas} - x_{H2O,gas,sat}(T'))\ c_{H2O,liq}\ T' + (x_{H2O,gas} - x_{H2O,gas,sat}(T'))\ r_{ice}(T)
\end{aligned} \qquad (29)$$

5.3.1 Simplifications

The model assumes also, that the condensation/evaporation process is related to a volume, which acts as mixing unit. This volume is defined by a certain pressure, density, temperature, humidity, CO_2 and water content. To overcome this dependence, a node has to introduce (see section 5.5). A node assures that the incoming mass flows are the outgoing mass flow. The node is defined by a pressure and can calculate e.g. the temperature T_{mix} with the knowledge of the incoming mass flows $\dot{m}_{air,in,i}$ and the temperatures $T_{in,i}$.

Each flow is also characterizes by its water vapor, CO_2 and water content, ($x_{H2O,gas,in,i}$, $x_{CO2,in,i}$, $x_{H2O,liq,in,i}$). From the known values the mixing temperature T_{mix} can be computed by using Equation 30.

$$T_{mix} = \frac{\sum_i \dot{m}_{air,in,i}\ (1 + x_{H2O,gas,in,i} + x_{CO2})\ T_{in,i}}{\sum_i \dot{m}_{air,in,i}\ (1 + x_{H2O,gas,in,i} + x_{CO2})} \qquad (30)$$

After this calculation all the values are known to use the condensation/evaporation model.

5.3.2 Algorithm

The algorithm of the condensation process can be discussed by means of the following situation. A small volume $V = 0.05\ m^3 = 50\ l$ pressurized of 101300 Pa is filled by air with a temperature of $T = 273.15$ K = 0°C. Hot air ($T_{in} = 303.15$ K = 30 °C) streams with a mass flow of $\dot{m}_{in} = 1$ kg/s into the volume. The outgoing mass flow $\dot{m}_{out}$ is also equal 1 kg/s. The humidity φ of both gas mixtures is assumed to be 100%. Within a time range of $dt = 0.01$s the temperature rise up to $T = 277.36$ K. After mixing the both gas quantities the mass of water vapor $m_{H2O,gas}$ reaches a value of 0.000464 kg. The saturation mass $m_{H2O,gas,sat}$ at the temperature T is 0.000299 kg. Under these conditions condensation occurs ($m_{H2O,gas,sat}(T) < m_{H2O,gas}$). In the following considerations m_{CO2} and $m_{H2O,liq}$ are set to zero. Under these conditions the solution of Equation 27 gives $T' = 280.44$ K.

Within a dynamically Simulink simulation the use of numerically solver function leads to heavy problems. At first the calculation time rises up and the real-time capability gets lost. Second the system stability is endangered. To overcome these problems the Equation 27 respectively Equation 29 have to be solved with am iterative while loop.

In each step i of the while loop a new value for T'_i can be calculated. Under the condition that the deviation between T'_i and $T'_{(i-1)}$ will be smaller than 0.1 K the while loop stops (see Equation 31).

$$\begin{gathered}\text{Break Condition :}\\ (T'_i - T'_{(i-1)}) < 0.1\,\text{K}\,,\, i = 1 \ldots N\,,\, T'_o = T\end{gathered} \tag{31}$$

In first approximation the relation $T'=T'_0=T$ is given. An adequate estimation for T'_i can be found by a simplified form of Equation 27 and a averaging between T'_i and $T'_{(i-1)}$ (see Equation 32).

$$\begin{gathered}T'_i = \frac{(c_{p,air} + x_{H2O,gas}\,c_{p,H2O,gas} + x_{CO2}\,c_{p,CO2})\,T + (x_{H2O,gas} - x_{H2O,gas,sat})\,r_0 + x_{H2O,liq}\,c_{H2O,liq}\,T - (x_{H2O,gas} - x_{H2O,gas,sat})\,r_{ice}(T)}{c_{p,air} + x_{H2O,gas,sat}\,c_{p,H2O,gas} + x_{CO2}\,c_{p,CO2} + (x_{H2O,liq} + x_{H2O,gas} - x_{H2O,gas,sat})\,c_{H2O,liq}}\\ x_{H2O,gas,sat} = x_{H2O,gas,sat}(T'_{(i-1)})\\ i = 1 \ldots N, T'_0 = T\\ T'_i = (T'_i - T'_{(i-1)})/2\end{gathered} \tag{32}$$

In the case described above the temperature T'_1 after the first loop is $T'_1 = 280.06$ K. The difference between T'_1 and $T = T'_0$ is 2.71 K. In the next loop a $T'_2 = 280.40$ K is calculated. In the third loop T'_3 has a value of 280.43, and the deviation of 0.03 K fulfill the break condition defined in Equation 31. The difference between T'_3 and the exact solution T' of Equation 27 is 0.01 K. The exact solution was evaluated by a Maple Script. The number of iteration until the break condition is reached, is dependant of the value of the volume, the mass flow and the humidity φ. As smaller the volume respectively as higher the mass flow or φ, as more number of iteration are necessary. Normally the number doesn't exceed three.

5.3.3 The Temperature

The equations Equation 18 … 21 are characteristic for a wet air flow. In several applications the temperature T_{air} has to be known. Knowing the temperature T and under assumption that the enthalpy flow of dry air flow is equal the enthalpy flow of the wet air. The temperature T_{air} can be calculated according to Equation 33.

$$T_{air} = \frac{(c_{p,air} + x_{H2O,gas}\ c_{p,H2O,gas})\ T + x_{H2O,gas}\ r_0}{(1 + x_{H2O,gas})\ c_{p,air}} \tag{33}$$

5.4 Flow Resistance

Table 6: Input and output variables of a flow resistance

Input Variables	**Output Variables**
Pressure	Pressure
Density	Density
Temperature	Temperature
Water Vapor Content	Mass Flow Dry Air
CO_2 Content	Water Vapor Content
Water Content	CO_2 Content
	Water Content

The dynamic of an air flow system is related to the velocity of the enthalpy flow. The enthalpy flow is defined by a mass flows $\dot{m}$, the temperature T and the specific heat capacity of the transported gas mixture (see Table 6). The transport of the gas through the system is defined by flow resistances. These components are linked to volume components respectively to components which are defined by pressure, density and temperature (see Figure 11). Using these input values, the parameter like density ρ_{FR} and temperature T_{FR} can be calculated (see Table 7).

Table 7: Operator modes of a flow resistance

$p_{out,1}$	=	$p_{in,2}$
$p_{out,2}$	=	$p_{in,1}$
Mode 0		
ρ_{FR}	=	$(\rho_{in,1}+\rho_{in,2})/2$
$x_{H2O,gas,FR}$	=	$(x_{H2O,gas,in,1}+x_{H2O,gas,in,2})/2$
$x_{CO2,FR}$	=	$(x_{CO2,in,1}+x_{CO2,in,2})/2$
$x_{H2O,liq,FR}$	=	$(x_{H2O,liq,in,1}+x_{H2O,liq,in,2})/2$
T_{FR}	=	$(T_{in,1}+T_{in,2})/2$
Mode 1		
ρ_{FR}	=	$\begin{Bmatrix} \rho_{in,1}, p_{in,1} \geq p_{in,2} \\ \rho_{in,2}, p_{in,2} > p_{in,1} \end{Bmatrix}$

$x_{H2O,gas,FR}$	=	$\begin{Bmatrix} x_{H2O,gas,in,1}, p_{in,1} \geq p_{in,2} \\ x_{H2O,gas,in,2}, p_{in,2} > p_{in,1} \end{Bmatrix}$
$x_{CO2,FR}$	=	$\begin{Bmatrix} x_{CO2,in,1}, p_{in,1} \geq p_{in,2} \\ x_{CO2,in,2}, p_{in,2} > p_{in,1} \end{Bmatrix}$
$x_{H2O,liq,FR}$	=	$\begin{Bmatrix} x_{H2O,liq,in,1}, p_{in,1} \geq p_{in,2} \\ x_{H2O,liq,in,2}, p_{in,2} > p_{in,1} \end{Bmatrix}$
T_{FR}	=	$\begin{Bmatrix} T_{in,1}, p_{in,1} \geq p_{in,2} \\ T_{in,2}, p_{in,2} > p_{in,1} \end{Bmatrix}$

The pressure inputs are cross linked to the outputs. The output 1 is defined by the pressure of input 2 and vice versa.

The mass flow $\dot{m}$ is combined with an average velocity v of the air-flow and the average density ρ_{FR} of gas mixture. The pressure drop Δp (see Figure 14) at the apertures pushes the gas through the flow component. The relationship between Δp and v respectively $\dot{m}$ is given by Equation 34.

$$\begin{aligned} v(t) &= \sqrt{\Delta p(t) \frac{2}{\rho_{FR}(t)} \frac{1}{\zeta_{total}(\mathrm{Re})}} \\ \dot{m}(t) &= A\, \rho_{FR}(t)\, v(t) \\ \dot{m}_{air}(t) &= \frac{\dot{m}(t)}{(1 + x_{H2O,gas,FR}(t) + x_{CO2,FR}(t))} \end{aligned} \tag{34}$$

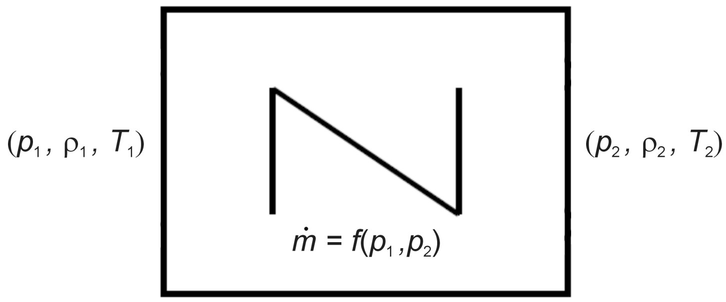

Figure 14: Inner structure of a flow resistance

A is the cross section of the flow resistance. In the Equation 33 density ρ_{FR} is assumed to stay constant over the whole length of the flow resistance. This assumption is only valid for incompressible flows. The average velocity is dependant of the minor loss coefficient ζ_{total}. ζ_{total} can be divided into the friction coefficient λ(Re) of the flow and into a minor loss coefficient ζ (see Equation 35). ζ is related to the design of the flow element.

$$\zeta_{total}(\mathrm{Re}) = \frac{L}{D} \lambda(\mathrm{Re}) + \zeta \tag{35}$$

D is the diameter and *L* the length of the flow element. The friction coefficient λ is a function of the Reynolds number Re (see Equation 36 and Figure 15). A duct model can be built up by a combination of flow resistances and volume elements (see Figure 8).

$$\text{Laminar Flow}: \lambda\,(\mathrm{Re}) = \frac{64}{\mathrm{Re}}\ ,\ \mathrm{Re} \leq 2320$$
$$\text{Turbulent Flow}: \lambda\,(\mathrm{Re}) = 0.3164\ \mathrm{Re}^{-0{,}25}\ ,\ \mathrm{Re} > 2320 \tag{36}$$
$$\text{Mixed Flow}: \lambda\,(\mathrm{Re}) = \begin{cases} \dfrac{64}{\mathrm{Re}}\ , & \mathrm{Re} \leq 1187.384382 \\ 0.3164\ \mathrm{Re}^{-0{,}25}\ , & \mathrm{Re} > 1187.384382 \end{cases}$$

The transition between laminar and turbulent flow shows a singularity. At the value Re = 2320 a gap occurs (Figure 15, black curve). This gap is no physical fact but is the result of the description by Equation 35. In the transition region Re can't be expressed by formula for λ(Re). For that reason a mixed flow curve (see Equation 36 and Figure 15, red curve) is defined.

In general flow resistance can't be described by analytically expression, but by a measured ζ_{total}(Re) curve. This matter of fact hasn't an impact in the next reflections.

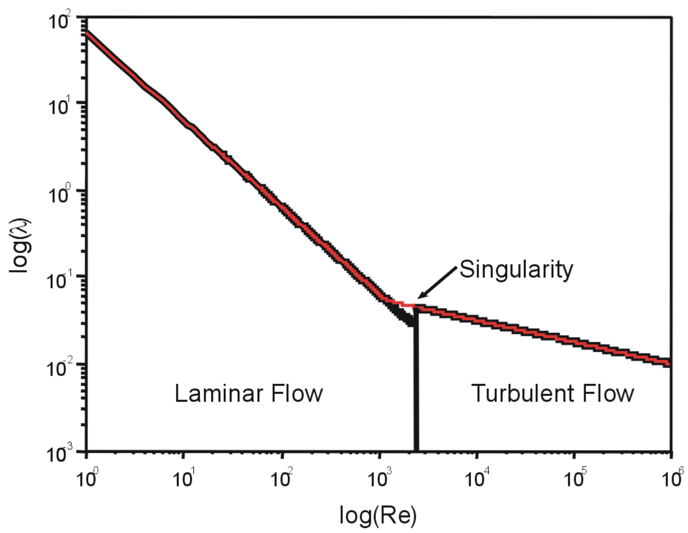

Figure 15: The transition between laminar and turbulent flow

The Reynolds number is dependant of the average velocity *v* (see Equation 37). η is the viscosity of air.

$$\mathrm{Re}(t) = \frac{v(t)\ D\ \rho\ (t)}{\eta} \tag{37}$$

The enthalpy flow $\dot{H}$, which is transferred through the flow resistance can compute with Equation 38.

$$\dot{H}(t) = \dot{m}(t)\,\bar{c}_p(t)\,T_{FR}(t) \tag{38}$$

5.4.1 Algorithm

The problem in solving the equations is related to the fact that the average flow velocity v is a function of the Reynolds number Re (see Equation 34). In turn Re is also a function of v (see Equation 37). A priori it isn't clear whether the flow can be described by a laminar or a turbulent characteristic. Therefore an iterative configuration under mixed flow conditions is built up. At the beginning of each time step of the dynamic simulations an initial value of Re_{init} and v_{init} has to be set to the value of the previous time step. Starting the simulation without knowing an accurate value for the velocity, asking for an estimation of v_{init} by using the Hagen-Poiseuille law (see Equation 39). The law of Hagen-Poiseuille bases on the assumption of laminar flow and cylindrical symmetry. Thus Re_{init} is only an approximation for the right value of Re. If $Re_0 = Re_{init}$ is smaller than 1187.384382 $v = v'_0$, and the iteration stops. Is Re_0 greater than 1187.384382 a v'_1 is calculated by Equation 39. With the new $v = v'_1$ a new Re_1 can be calculated.

$$\begin{aligned} v'_0 &= v_{init} = \frac{(D/2)^2\,\Delta p}{8\eta\;L} \\ \mathrm{Re}_0 &= \mathrm{Re}_{\mathrm{init}} = \frac{v'_0\,D\,\rho_{FR}}{\eta} \\ v'_i &= \sqrt{\Delta p\,\frac{2}{\rho}\,\frac{1}{\zeta_{total}(\mathrm{Re}_{\mathrm{i-1}})}} \\ \mathrm{Re}_{\mathrm{i}} &= \frac{v'_i\,D\,\rho_{FR}}{\eta} \end{aligned} \tag{39}$$

This loop is executed till the condition Equation 40 is satisfied.

$$\left|v'_i - v'_{i-1}\right| < 0.001\,v'_{i-1} \tag{40}$$

5.5 The Node

Table 8: Input and output variables of a node

Input Variables	**Output Variables**
Pressure	Pressure
Density	Density
Temperature	Temperature
Mass Flow Dry Air	Water Vapor Content
Water Vapor Content	CO_2 Content
CO_2 Content	Water Content
Water Content	

The node is characterized by the fact, that the sum of the incoming flows is equal the sum of the outgoing flows (see Equation 40).

$$\sum_i \dot{m}_{in,i} - \sum_j \dot{m}_{out,j} = 0 \tag{40}$$

The node itself has undefined volume, therefore the pressure is estimated by using Equation 40. The incoming flows define the values for temperature, density, water vapor, CO_2 and water content. The average values are calculated by weighting with the mass flows (see Equation 30). The function of a node can be discussed with help of an example (see Figure 16). In general the node is linked between to flow resistances. Each flow resistance needs defined pressures at both ends. The node in contrast needs a defined mass flows to calculate a pressure.

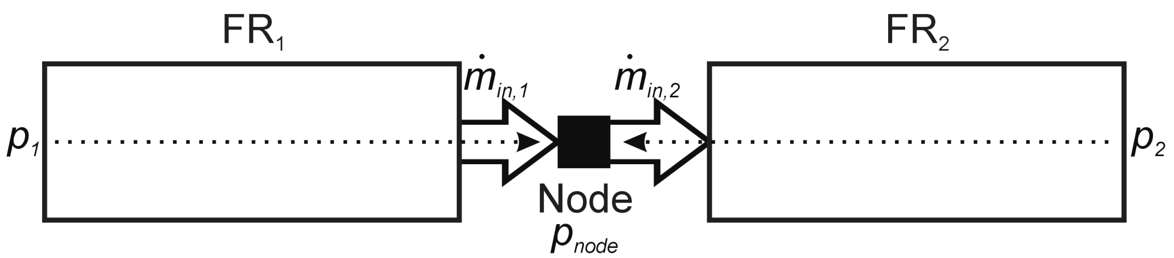

Figure 16: Node between to flow resistance (FR)

Therefore the node has to be initialized with a $p_{node} = p_{node,init}$. At the start of the simulation with help of $p_{node,init}$ the two flow resistance can compute a mass flow. All the important parameter like mass flow and pressure are transferred to the node (see Figure 16). The flow resistance has calculated the mass flow by Equation 34, therefore the relation between the mass flow and the pressure drop isn't linear. In the node a linearization step occurs (see Equation 41).

$$\begin{aligned} \dot{m}_{in,1}(t) &= K_1(t) \cdot (p_1(t) - p_{node}) \\ \dot{m}_{in,2}(t) &= K_2(t) \cdot (p_2(t) - p_{node}) \end{aligned} \tag{41}$$

The linearization constants K_1 and K_2 are time dependant, from one to the next time step the values change. This linear form can insert in the equation Equation 40 and p_{node} can be computed (see Equation 42).

$$p_{node} = \frac{K_1(t)\ p_1(t) + K_2(t)\ p_2(t)}{K_1(t) + K_2(t)} \tag{42}$$

The equations above describe the case for one incoming respectively one outgoing mass flow. But in general the node isn't limited in the number of mass flows.

5.5.1 The Dynamic of the Node

The node shows a certain dynamic. This dynamical effect isn't related to a physical behavior. But is correlated to the fact, that the calculation of p_{node} is only a estimation of the real value. It isn't assured, that the two flow resistance calculate with the p_{node} in the next time step an equal mass flow. The transient response of the node last longer all the more the flow velocities differ. Therefore the lengths respectively the diameter of the flow resistances have an influence of the transient response. The node runs more stable, if both flow resistances have the same parameter

5.6 Valve

Table 9: Input and output variables of a valve

Input Variables	**Output Variables**
Pressure	Pressure
Density	Density
Temperature	Temperature
Mass Flow Dry Air	Mass Flow Air
Water Vapor Content	Water Vapor Content
CO_2 Content	CO_2 Content
Water Content	Water Content

In the following two different types of valves will be discussed. At first valves will be shown, which assume incompressible flow, and second valves, which assume compressible flow.

5.6.1 Incompressible Flow

A valve is characterized by a drag factor ζ. This factor ζ is constant. Is the valve linked to volumes, the important inputs are the pressures. Is the pressure drop defined, the mass flow through the valve can be calculated (see Equation 43).

$$\begin{aligned} v(t) &= \sqrt{\Delta p(t) \frac{2}{\rho_{valve}(t)} \frac{1}{1+\zeta}} \\ \dot{m}(t) &= A \, \rho_{valve}(t) \, v(t) \end{aligned} \tag{43}$$

The variable like density and temperature of the valve are always defined by the volume with the higher pressure or the incoming flow (see Table 7, Mode 1). The cross section A of the valve isn't a constant value, but can be changed during the simulation. As parameter get the valve the maximum effective area A_{max}. If the throttle is parallel to the flow direction the valve is open. If the throttle is perpendicular orientated to the flow direction the valve is closed (see Figure 17).

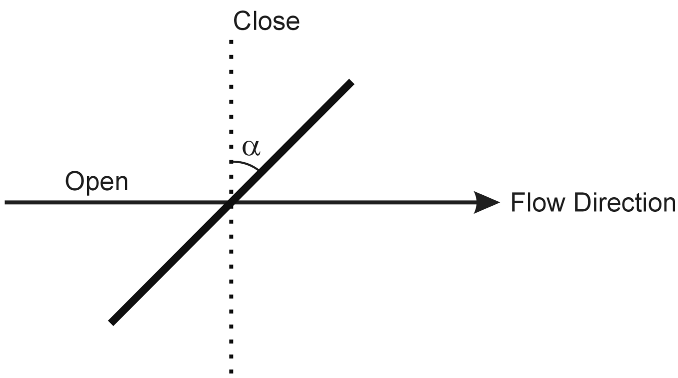

Figure 17: The position of the throttle of a valve

The opening is characterized by the opening angel α. For a certain aperture between the close and open state the effective cress section A is given by equation Equation 44.

$$A = A_{max} \sin(\alpha) \tag{44}$$

The equations Equation 43 and Equation 44 are sufficient to define the configuration valve and two volumes. In the other configuration the valve is located between a flow resistance and a volume (see Figure 18). The valve pressure p_{valve} (see Figure 18) is defined by the pressure of the volume. The mass flow $\dot{m}_{valve}$ through the valve is defined by the mass flow of the flow resistance $\dot{m}$ (see Equation 45).

$$\dot{m}_{valve} = \sin(\alpha)\,\dot{m} \tag{45}$$

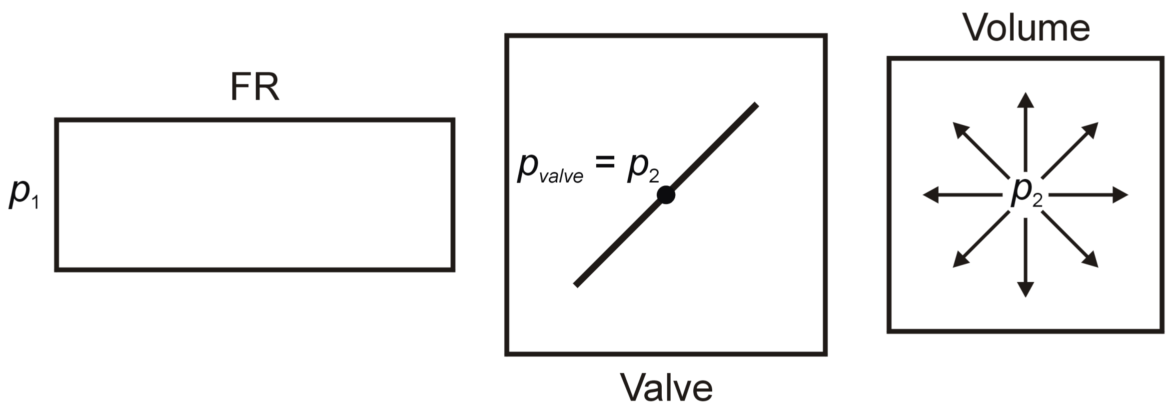

Figure 18: Configuration Valve and two flow resistances

5.6.2 Compressible Flow

Within a valve with compressible flow properties, the density can change. Under the assumption, that adiabatic compression respectively adiabatic expansion occurs, the relations between the static values and the total values are given by the Equation 46.

$$\frac{p}{p_{total}} = \left(\frac{\rho}{\rho_{total}}\right)^{\gamma} = \left(\frac{T}{T_{total}}\right)^{\frac{\gamma}{\gamma-1}} \tag{46}$$

γ is defined as ratio c_p / c_v. The total temperature T_{total} is given by the enthalpy equation of the flow (see Equation 47).

$$\begin{aligned} m\, c_p\, T_{total} &= m\, c_p\, T + \frac{m}{2} v^2 \\ &\Downarrow \\ T_{total} &= T + \frac{1}{2\, c_p} v^2 \\ &\Downarrow \\ T_{total} &= T\, (1 + \frac{\gamma - 1}{2} \mathrm{Ma}^2) \end{aligned} \tag{47}$$

$$\text{Mach Number} : \mathrm{Ma} = \frac{v}{a}, \text{Sonic Speed} : a = \sqrt{\gamma\; R\, T}$$

The relation between T and T_{total} can be included in Equation 46 (see Equation 48).

$$\begin{aligned} \frac{p}{p_{total}} &= (1 + \frac{\gamma - 1}{2} \mathrm{Ma}^2)^{-\frac{\gamma}{\gamma-1}} \\ \frac{\rho}{\rho_{total}} &= (1 + \frac{\gamma - 1}{2} \mathrm{Ma}^2)^{-\frac{1}{\gamma-1}} \\ \frac{T}{T_{total}} &= (1 + \frac{\gamma - 1}{2} \mathrm{Ma}^2)^{-1} \end{aligned} \tag{48}$$

These equations are based on the conservation of mass, momentum and energy. With help of Equation 48 the compressible mass flow equation can be developed (see Equation 49).

$$\dot{m} = \frac{A\, p_{total}}{\sqrt{T_{total}}} \sqrt{\frac{\gamma}{R}}\, \mathrm{Ma}\, (1 + \frac{\gamma - 1}{2} \mathrm{Ma}^2)^{-\frac{\gamma+1}{2(\gamma-1)}} \tag{49}$$

The Equation 49 can be used to build up an algorithm for a valve with compressible flow properties. Equation 50 is used to calculate the Mach number Ma. Temperature T_{total} and pressure p_{total} are defined by the volume with the highest pressure.

$$\mathrm{Ma} = \sqrt{\frac{2}{\gamma - 1}\left(\left(\frac{p_{total}}{p}\right)^{\frac{(\gamma-1)}{\gamma}} - 1\right)} \tag{50}$$

The Mach number characteristics based on Equation 50 is shown in Figure 19, (light grey curve). In general the Mach number doesn't exceed a maximum value of 1 (see Figure 19, black curve). In the case of air Ma = 1 is reached at a pressure ratio $p^*/p_{total} = (2/(\gamma+1))^{\gamma/(\gamma-1)} = 0.53$.

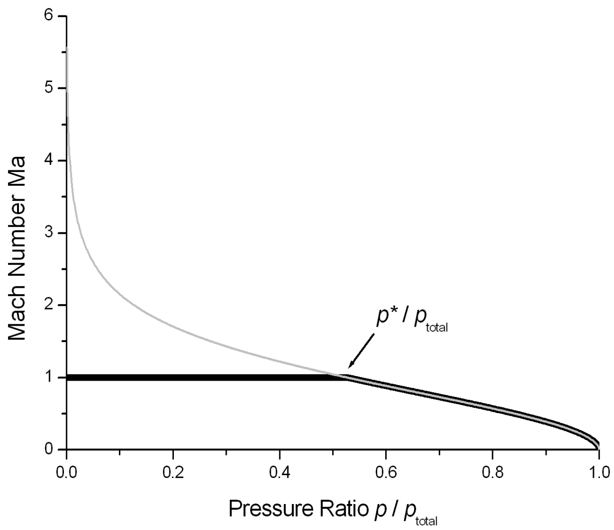

Figure 19: Mach number characteristics based on Equation 50

5.7 Heat Exchanger

5.7.1 Heat Transfer Units

Table 10: Input and output variables of a heat transfer unit

Input Variables	Output Variables
Temperature	Temperature
	Heat Transfer Rate

Heat transfer units play an important part inside the heat exchanger. Three different heat transfer processes will be discussed, the conduction, the convection and the radiation of heat.

The conduction can be described by a thermal conductivity λ [W/m K]. The heat is transferred from a medium with the temperature T_1 through a heat conductor with a surface A and a thickness L to a medium with a temperature T_2 (see Figure 20). The heat transfer rate can be expressed by Equation 51.

$$\dot{Q}_{cond} = \lambda \; A \frac{T_1 - T_2}{L}. \tag{51}$$

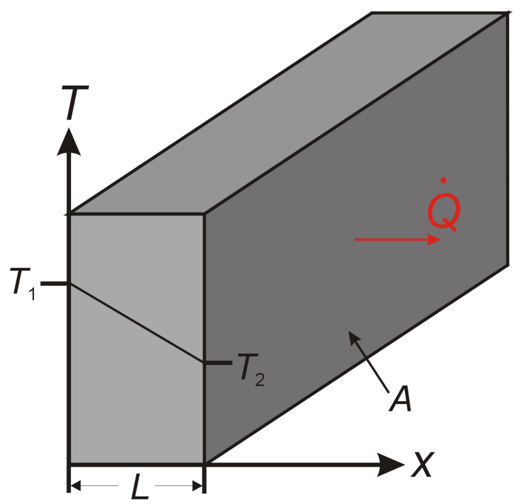

Figure 20: Heat conduction

The convection can be described by the convection heat transfer coefficient α [W/m^2 K]. Heats is transferred from a medium with the temperature T_1 to a surface A with temperature T_s and back from the surface to a medium with a temperature T_2 (see Figure 21). The heat transfer rates can be expressed by Equation 52.

$$\dot{Q}_{conv,1} = \alpha_1 \; A \, (T_s - T_1)$$
$$\dot{Q}_{conv,2} = \alpha_2 \; A \, (T_s - T_2)$$
$$\frac{dT_s}{dt} = \frac{\dot{Q}_{conv,1} + \dot{Q}_{conv,2}}{m \, c} \qquad (52)$$

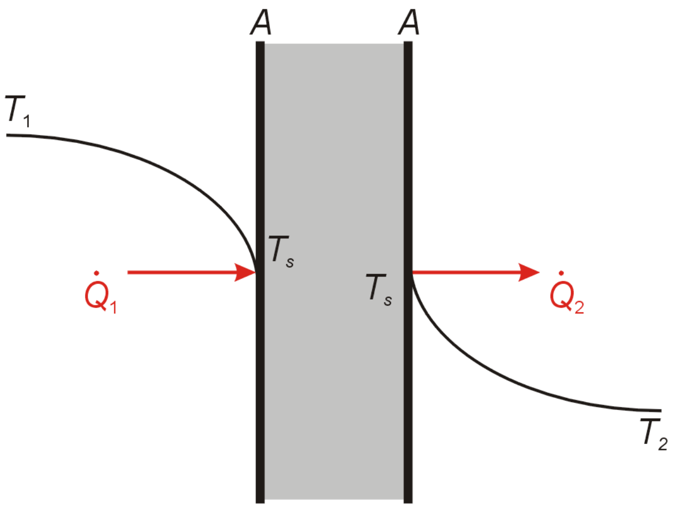

Figure 21: Heat convection

The modification of the surface temperature is given by Equation 53. The heat capacity of the transfer wall is the product of the specific heat capacity *c* and the mass *m*.

The radiation process can be described by the Stefan-Boltzmann constant $\sigma = 5.67\ 10^{-8}$ W/m^2 K and the emissity ε, $0 \leq \varepsilon \leq 1$. The heat is transferred from a surface with the temperature T_s to a gas with the temperature T (see Figure 22). The heat transfer rate can be expressed by Equation 53.

$$Q_{dot}^{Rad} = \varepsilon \cdot \sigma \cdot A \cdot (T_s^{\,4} - T^4) \qquad (53)$$

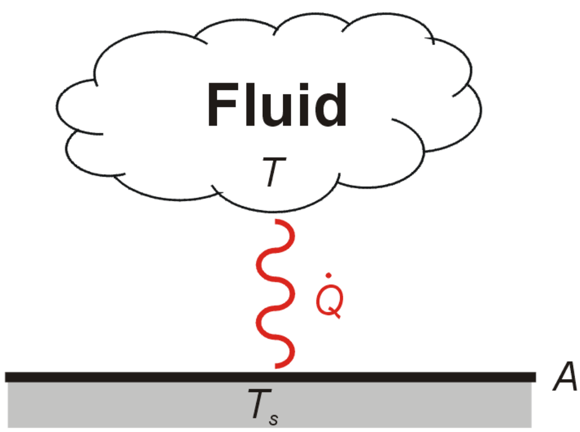

Figure 22: Heat radiation

Inside a duct model heat transfer between the air and the surrounding area via the duct wall and the isolation can be calculated. Knowing the flow velocity v respectively the Reynolds number Re, the Nusselt number Nu respectively convection heat transfer coefficient the can be determined using Equation 54.

$$\mathrm{Nu} = (3.66^3 + 1.66^3 \ \mathrm{Re}\ \mathrm{Pr}\ \frac{D_{duct}}{L_{duct}})^{1/3}, \text{Laminar Flow}$$

$$\mathrm{Nu} = 0.012\ (\mathrm{Re}^{0.87} - 280)\ \mathrm{Pr}^{0.4}\ (1 + \frac{D_{duct}}{L_{duct}})^{2/3}\ , \text{Turbulent Flow}$$

$$\lambda_{air} = 0.00452 + 7.2828210^{-5}\ T \tag{54}$$

$$\mathrm{Pr} = \frac{\eta_{air}\ c_{air}}{\lambda_{air}}$$

$$Nu = \frac{\alpha_{air}\ D_{duct}}{\lambda_{air}}$$

The Prandtl number Pr is a relation of the dynamic viscosity η, the specific heat capacity c_p and the thermal conductivity λ. The Nusselt number Nu is a relation of the convection heat transfer coefficient α, the Diameter of the duct D_{duct}. The thermal conductivity is a function of the air temperature T.

The overall heat transfer can be computed by Equation 55. The convection heat transfer coefficient of the wall and the isolation are user defined parameters. b_{wall} is the is the thickness of the wall and $b_{isolation}$ is the thickness of the isolation.

$$\dot{Q}_{air,ambient} = \frac{A_{wall}\ (T - T_{ambient})}{(1/\alpha_{air}) + (1/\alpha_{wall}) + (1/\alpha_{isolation})}$$

$$\alpha_{wall} = \frac{\lambda_{wall}}{b_{wall}} \tag{55}$$

$$\alpha_{isolation} = \frac{\lambda_{isolation}}{b_{isolation}}$$

5.7.2 Steady State Description of a Heat Exchanger

Table 11: Input and output variables of a heat exchanger

Input Variables	**Output Variables**
Pressure	Pressure
Density	Density
Temperature	Temperature
Water Vapor Content	Mass Flow Dry Air
CO_2 Content	Water Vapor Content
Water Content	CO_2 Content
	Water Content

Within a heat exchanger heat is transferred from the hot side towards the cold side (see Figure 23).

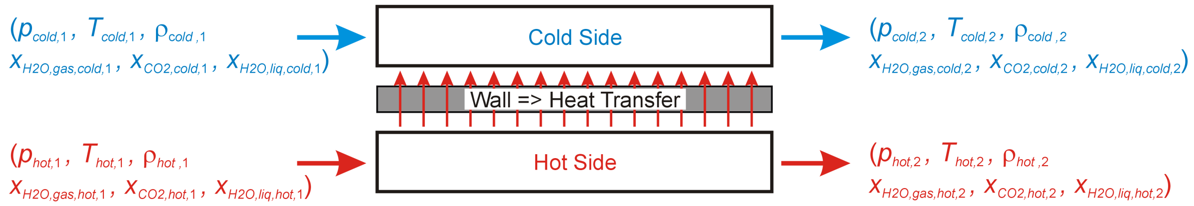

Figure 23: Basic configuration of a heat exchanger

Knowing the pressure drop the mass flow through the heat exchanger can be calculated with help of Equation 56 (see Figure 23).

$$\begin{aligned}
\dot{m}_{air,cold} &= \left(\frac{(p_{cold,1} - p_{cold,2})}{K_{cold,1}} \frac{\rho_{air,cold,1}}{\rho_0} \right)^{\frac{1}{m_{cold,1}}}, \ p_{cold,1} > p_{cold,2} \\
\dot{m}_{air,hot} &= \left(\frac{(p_{hot,1} - p_{hot,2})}{K_{hot,1}} \frac{\rho_{air,hot,1}}{\rho_0} \right)^{\frac{1}{m_{hot,1}}}, \ p_{hot,1} > p_{hot,2}
\end{aligned} \tag{56}$$

K_1 and m_1 are characteristic parameters of a heat exchanger. ρ_0 is the density under standard ISA (ISA: *International Standard Atmosphere*) conditions (p_0 =101300 Pa, T_0 = 288.15 K = 15 °C, ρ_0 = 1.225 kg/m³). The state variables of the heat exchanger are always defined by the input with the highest pressure (see Table 7, Mode 1)

The heat transfer is expressed by an efficiency η. The efficiency η is defined as ratio between them real heat transfer rate $\dot{Q}_{real}$ and the maximal possible heat transfer rate $\dot{Q}_{max}$ (see Equation 57) .

$$\eta = \frac{\dot{Q}_{real}(\dot{m}_{air,hot})}{\dot{Q}_{max}(\dot{m}_{air,hot})} \tag{57}$$

The efficiency is a function of the mass flow. The incoming and outgoing mass flows on the cold side respectively the hot side, are assumed to be equal. Therefore the following enthalpy flows enter and leave the system (see Equation 58).

$$\begin{aligned}
\dot{H}_{cold,in} &= \dot{m}_{cold}\ \bar{c}_{p,cold}\ T_{cold,in} \\
\dot{H}_{hot,in} &= \dot{m}_{hot}\ \bar{c}_{p,hot}\ T_{hot,in} \\
\dot{H}_{cold,out} &= \dot{m}_{cold}\ \bar{c}_{p,cold}\ T_{cold,out} \\
H_{hot,out} &= \dot{m}_{hot}\ \bar{c}_{p,hot}\ T_{hot,out}
\end{aligned} \tag{58}$$

$$\begin{aligned}
\dot{m}_{cold} &= \dot{m}_{air,cold}\ (1 + x_{H2O,gas,cold} + x_{CO2,cold}) \\
\dot{m}_{hot} &= \dot{m}_{air,hot}\ (1 + x_{H2O,gas,hot} + x_{CO2,hot})
\end{aligned}$$

Under static conditions the conservation of enthalpy has to be fulfilled (see Equation 59).

$$\dot{H}_{cold,in} + \dot{H}_{hot,in} = \dot{H}_{cold,out} + \dot{H}_{hot,out} \tag{59}$$

Under the assumption of an efficiency $\eta = 1$ and a counter flow respectively a cross flow configuration of the heat exchanger (see Figure 24, see Equation 60a), the outgoing temperature $T_{hot,out}$ of the hot side is equal the incoming temperature of the cold side $T_{cold,in}$. Under the assumption of an a parallel flow configuration (see Figure 24, Equation 60b) the outgoing temperature $T_{hot,out}$ is equal the outgoing temperature of the cold side $T_{cold,out}$. Using Equation 57 the maximal heat transfer rate $\dot{Q}_{max}$ can be calculated.

$$\dot{Q}_{max} = \dot{m}_{hot}\ \bar{c}_{p,hot}\left(T_{hot,in} - T_{cold,in}\right) \tag{60a}$$

$$\dot{Q}_{max} = \left(T_{hot,in} - T_{cold,in}\right)\frac{\dot{m}_{cold}\ \dot{m}_{hot}\ \bar{c}_{p,cold}\ \bar{c}_{p,hot}}{\dot{m}_{cold}\ \bar{c}_{p,cold} + \dot{m}_{hot}\ \bar{c}_{p,hot}} \tag{60b}$$

With the efficiency η maximal heat transfer rate can be projected to the realistic heat transfer rate $\dot{Q}_{real}$ (see Equation 55). Knowing $\dot{Q}_{real}$ the real outgoing temperatures can be computed (see Equation 61).

$$T_{cold,out} = T_{cold,in} + \frac{\dot{Q}_{real}}{\dot{m}_{cold}\ c_{p,cold}}$$
$$T_{hot,out} = T_{hot,in} - \frac{\dot{Q}_{real}}{\dot{m}_{hot}\ c_{p,hot}} \quad (61)$$

The steady state description delivers the real temperature, but isn't adapted to figure out the dynamic of the heat exchanger.

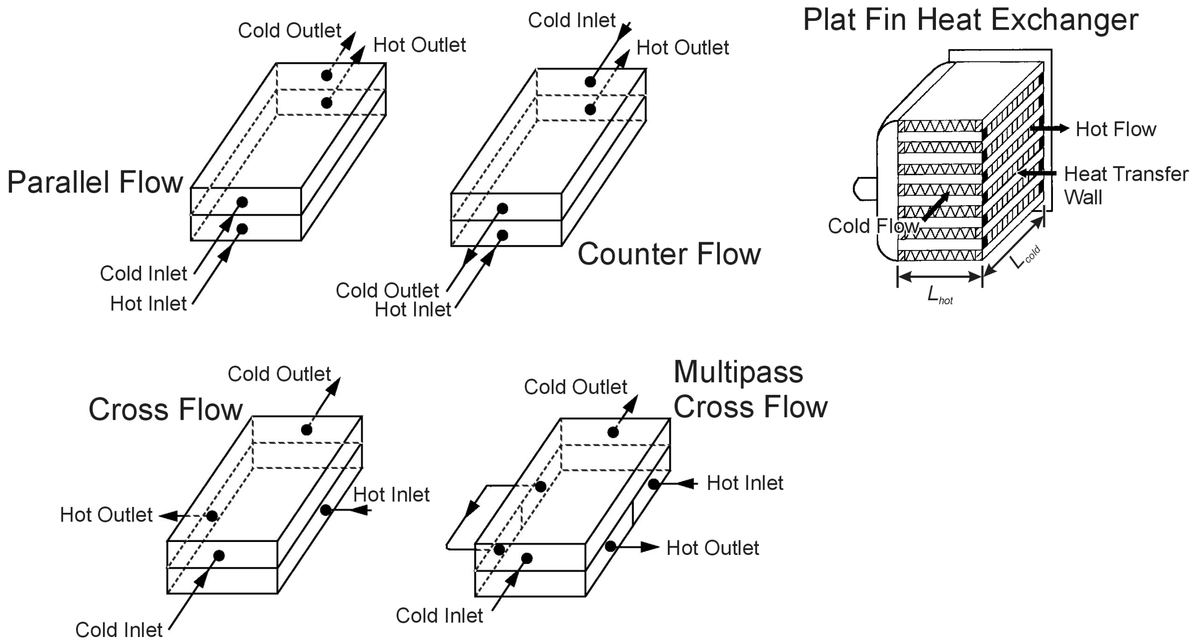

Figure 24: Different configuration of heat exchangers (**Allied-Signal 1990**)

In general the heat exchanger can't be described with a constant efficiency η, but the efficiency is a function of the mass flow of the dry air through the cold respectively the hot side (see Figure 25).

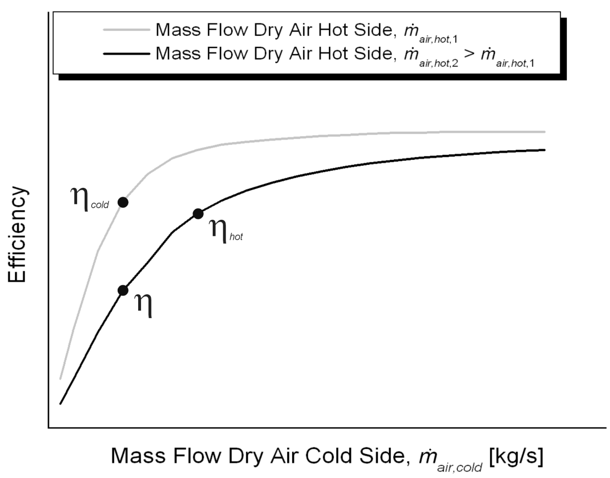

Figure 25: Efficiency function of a heat exchanger

5.7.3 Dynamical Description of a Heat Exchanger

The dynamical behavior of a heat exchanger can be simulated by a combination of duct elements and a heat transfer unit described above (see Figure 26). The cold and the hot side of the heat exchanger are displayed by two ducts. The heat transfer occurs over a convection heat transfer unit. By the heat transfer the hot side is cooled down, and the cold side is heated up.

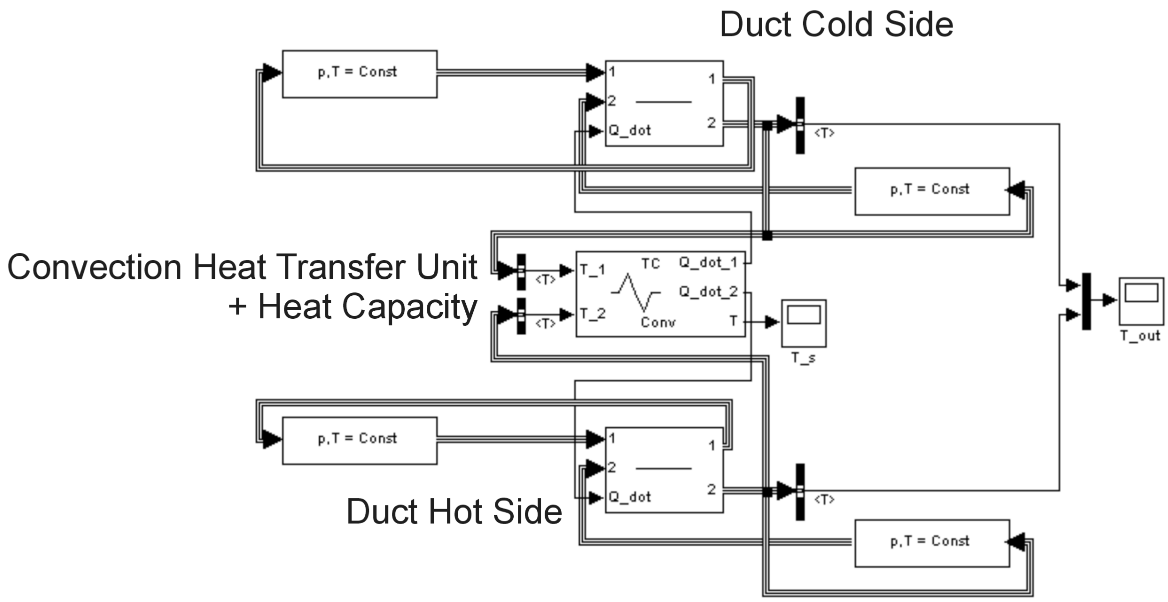

Figure 26: Dynamical Heat Exchanger consisting of two ducts and a convection heat transfer unit with heat capacity

The Simulink model of a dynamic heat exchanger shown in Figure 23 can only be used to rebuild heat exchanger in parallel flow configuration (see Figure 23).

In industrial applications heat exchanger in parallel flow configuration are not be used by reason of their lower efficiency. Therefore heat exchangers in counter flow respectively a cross flow configuration have to be described with another algorithm.

This algorithm is related to the steady state algorithm. In the following consideration the heat transfer factor $F_{\alpha A} = \alpha A$ has to be estimated. The convection heat transfer coefficient α is a function of the flow velocity v (see Equation 54). Decreasing flow velocity is related to a decreasing α, therefore two different cases have to be distinguished.

$\dot{m}_{cold} \rightarrow 0$: Decreasing mass flow respectively flow velocity is related to decreasing efficiencies (see Figure 25).

$\dot{m}_{hot} > \dot{m}_{cold}$: In the case, that $\dot{m}_{hot}$ is larger then $\dot{m}_{cold}$, the heat transfer is limited by the cold side. According to Equation 57 and 60a the transferred heat $\dot{Q}_{real}$ linear dependant to the mass flow $\dot{m}_{hot}$. Assuring that $T_{cold,out}$ is always smaller than $T_{hot,in}$ the efficiency has to become smaller (see Equation 61).

Based on this consideration in general the efficincy η is a function of the mass flow and the corresponding heat transfer factors ($\eta = f(\dot{m}_{hot}, \dot{m}_{cold}, F_{\alpha A,hot}, F_{\alpha A,cold})$). Only in the case $\dot{m}_{hot} = \dot{m}_{cold}$ the efficiency η is exclusively a function of the heat transfer factors ($\dot{m}_{hot} = \dot{m}_{cold} \Rightarrow \eta = f(F_{\alpha A,hot}, F_{\alpha A,cold})$). Below the heat exchanger is defined by the tuple $(\dot{m}_{hot}, T_{hot,in}, \dot{m}_{cold}, T_{cold,in})$, $\dot{m}_{hot} \neq \dot{m}_{cold}$.

Factor $F_{\alpha A}$, hot side: The tuple $(\dot{m}_{hot}, T_{hot,in}, \dot{m}_{cold}, T_{cold,in})$ is projected onto the case $\dot{m}_{cold} = \dot{m}_{hot}$. In that case the efficiency η_{hot} can be read off form the efficiency (see Figure 25).

The heat transfer occurs over the contact surface A_{hot}. L_{hot} is the contact length in flow direction (see Figure 24, Plat Fin Heat Exchanger). Along the contact length the Temperature profile $T_{hot}(x)$, $0 \leq x \leq L_{hot}$ is formed (see Figure 27a, see Equation 62).

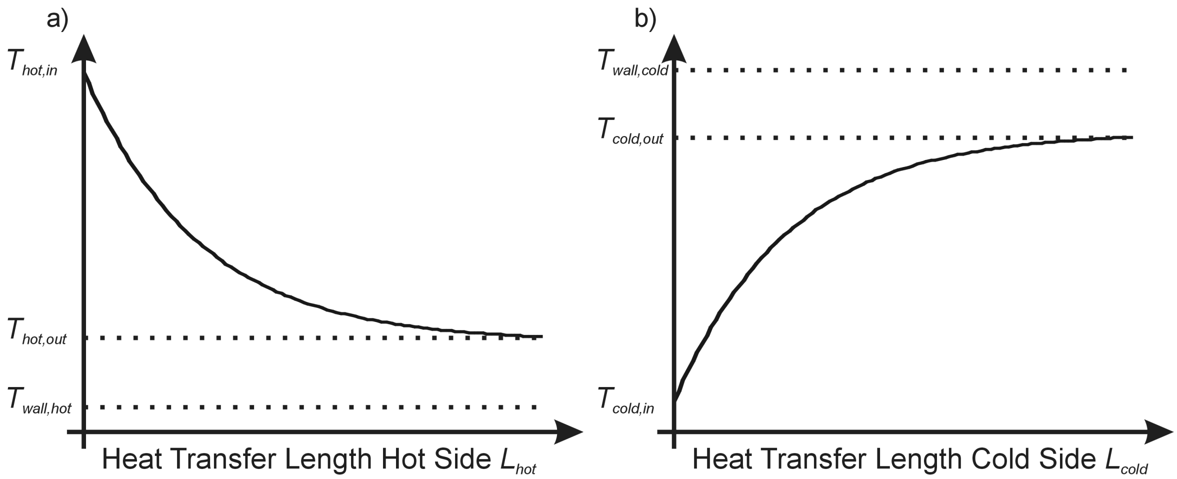

Figure 27: a) Hot side: Temperature profile along the contact length
b) Cold side: Temperature profile along the contact length

The temperature profile is derived from the differential equation for a heat transfer air – wall (see equation 62). Knowing η_{hot} the superscript $a_{hot} = \alpha_{hot} A_{hot} / \dot{m}_{hot} \bar{c}_{p,hot}$ can be determined. Using $F_{\alpha A,hot} = \alpha_{hot} A_{hot}$ the transferred heat $\dot{Q}_{wall,hotm}$ can be calculated.

$$\dot{m}_{hot}\ \bar{c}_{p,hot}\ L_{hot}\ \frac{dT_{hot}(x)}{dx} = \alpha_{hot}\ A_{hot}\ (T_{hot}(x) - T_{wall,hot})$$
$$\Rightarrow\ T_{hot}(x) = T_{wall,hot} + \left[T_{hot,in} - T_{wall,hot}\right] \exp(-a_{hot}\ \frac{x}{L_{hot}})$$

$$\begin{gathered}\eta_{hot} = \frac{T_{hot,in} - T_{hot}(L_{hot})}{T_{hot,in} - T_{cold,in}} \\ \text{Assumption}: T_{wall,hot} = T_{cold,in} \\ \Rightarrow\ a_{hot} = -\ln(1-\eta_{hot}) = \frac{\alpha_{hot}\ A_{hot}}{\dot{m}_{hot}\ \bar{c}_{p,hot}} = \frac{F_{\alpha A,hot}}{\dot{m}_{hot}\ \bar{c}_{p,hot}}\end{gathered} \tag{62}$$

$$\bar{T}_{hot} = T_{wall,hot} + (T_{hot,in} - T_{wall,hot})\ (1 - e^{-a_{hot}})/a_{hot}$$
$$\Rightarrow\ \dot{Q}_{wall,hot} = F_{\alpha A,hot}\ (T_{wall,hot} - \bar{T}_{hot})$$

Factor $F_{\alpha A}$, cold side: The calculation of $\alpha_{cold}\,A_{cold}$ follows analogous considerations (see above). The tuple $(\dot{m}_{hot}, T_{hot,in}, \dot{m}_{cold}, T_{cold,in})$ is projected onto the case $\dot{m}_{hot} = \dot{m}_{cold}$ respectively the efficiency η_{cold} (see Figure 25). The temperature profile $T_{cold}(x)$, $0 \le x \le L_{cold}$ is shown in Figure 27b.

$$\dot{m}_{cold}\ \bar{c}_{p,cold}\ L_{cold}\ \frac{dT_{cold}(x)}{dx} = \alpha_{cold}\ A_{cold}\ (T_{cold}(x) - T_{wall,cold})$$
$$\Rightarrow\ T_{cold}(x) = T_{wall,cold} + \left[T_{cold,in} - T_{wall,cold}\right] \exp(-a_{cold}\ \frac{x}{L_{cold}})$$

$$\begin{gathered}\eta_{cold} = \frac{T_{cold,in} - T_{cold}(L_{cold})}{T_{cold,in} - T_{hot,in}} \\ \text{Assumption}: T_{wall,cold} = T_{hot,in} \\ \Rightarrow\ a_{cold} = -\ln(1-\eta_{cold}) = \frac{\alpha_{cold}\ A_{cold}}{\dot{m}_{cold}\ \bar{c}_{p,cold}} = \frac{F_{\alpha A,cold}}{\dot{m}_{cold}\ \bar{c}_{p,cold}}\end{gathered} \tag{63}$$

$$\bar{T}_{cold} = T_{wall,cold} + (T_{cold,in} - T_{wall,cold})(1 - e^{-a_{cold}})/a_{cold}$$
$$\Rightarrow\ \dot{Q}_{wall,cold} = F_{\alpha A,cold}\ (T_{wall,cold} - \bar{T}_{cold})$$

The heat transfer wall is defined by m_{wall} and a specific heat capacity c_{wall}. Using Equation 64 the modifications of the wall temperatures $T_{wall,hot}$ respectively $T_{wall,cold}$ can be calculated.

$$
\begin{aligned}
\frac{dT_{wall,hot}(t)}{dt} &= \frac{\dot{Q}_{wall,hot}}{m_{wall}\ c_{wall}} \\
\frac{dT_{wall,cold}(t)}{dt} &= \frac{\dot{Q}_{wall,cold}}{m_{wall}\ c_{wall}}
\end{aligned}
\tag{64}
$$

Algorithm: Within the algorithm different heat exchanger types like plat fin (see Figure 24) or tubular heat exchanger will be distinguished. The different types are defined by efficiency maps (see Figure 25). The dynamic of a heat exchanger is specified by the heat capacity of the wall. The algorithm is working with two independent wall temperatures $T_{wall,hot}$ and $T_{wall,cold}$. By this means in the static equilibrium the same end values will be reached like in the case of steady state definition of a heat exchanger. Additional the algorithm ensure real time capability and a high degree of stability. In reality the heat transfer wall is characterized by only one average value of the wall temperature $\overline{T}_{wall}$ respectively a temperature profile. Therefore only a good approximation of the response time is given.

5.8 Fan

Table 12: Input and output variables of a fan

Input Variables	Output Variables
Pressure	Pressure
Density	Density
Temperature	Temperature
Water Vapor Content	Mass Flow Dry Air
CO_2 Content	Water Vapor Content
Water Content	CO_2 Content
	Water Content

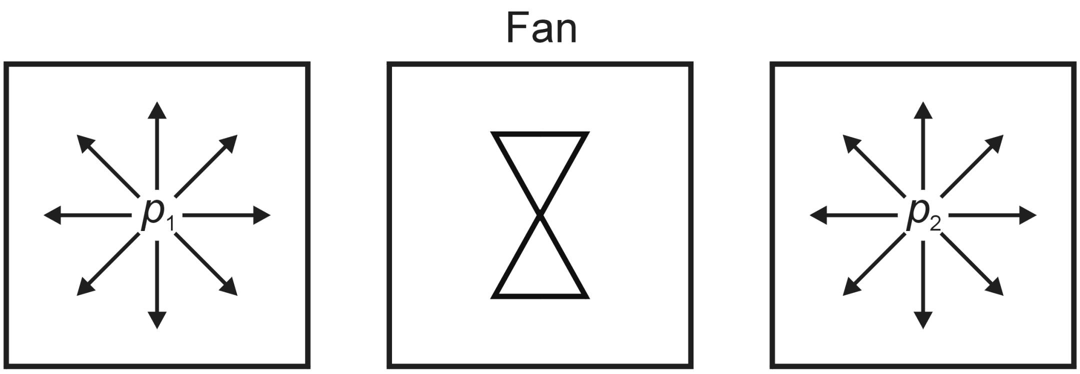

Figure 28: Configuration of a fan component as flow resistance

The fan element is described as flow resistance (see Figure 28). By a given pressure drop Δp between the inlet and the outlet and a rotational speed n the volume flow $\dot{V}$ can be calculated (see Figure 29a). The fan elements are divided in two different model classes. A generalized fan is defined with help of Equation 65. To evaluate the mass flow the cubic equation has to be solved with the method of Cordano.

The characteristic map of a fan is divided in a stable region and instable region (see Figure 29). For a given rotational speed n a defined maximal pressure drop Δp_{max} is possible. Theoretically for a given pressure ratio two different volume flows are feasible. In the stable mode only the higher volume flow is reachable value. The algorithm can be divided in three operation modes (see Equation 65 and Figure 29), the normal mode ($\Delta p < \Delta p_{max}$), the linear scaling ($\Delta p > \Delta p_{max}$) and the logarithmic scaling ($|\dot{V}| > |\dot{V}_{limit}|$). The density ρ_0 can be calculated by ISA conditions. The rotational speed is normalized on n_0.

$$\rho = \frac{\rho_{inlet} + \rho_{inlet}\,(p_{outlet} / p_{inlet})^{\frac{1}{\gamma}}}{2}$$

$$\rho_{outlet} = \rho_{inlet}\,(p_{outlet} / p_{inlet})^{\frac{1}{\gamma}}$$

$$T_{out} = T_{in}\,(p_{outlet} / p_{inlet})^{\frac{\gamma-1}{\gamma}}$$

$$p_1 > p_2 : p_{inlet} = p_1 , p_{outlet} = p_2 , \rho_{inlet} = \rho_1 , T_{inlet} = T_1$$
$$p_2 > p_1 : p_{inlet} = p_2 , p_{outlet} = p_1 , \rho_{inlet} = \rho_2 , T_{inlet} = T_2$$

$$\text{Normal Mode} : \Delta p < \Delta p_{max}$$
$$\Delta p = A_3 \dot{V}^3 + A_2 \dot{V}^2 + A_1 \dot{V} + A_0$$
$$\rightarrow \dot{V} = f(\Delta p)\ (\leftrightarrow \text{ Method of Cordano})$$
$$\dot{m} = \rho \dot{V}$$

$$\begin{aligned} A_0 &= (\rho / \rho_0)\, a_0\, (n / n_0)^2 \\ A_1 &= (\rho / \rho_0)\, a_1\, (n / n_0)^1 \\ A_2 &= (\rho / \rho_0)\, a_2\, (n / n_0)^0 \\ A_3 &= (\rho / \rho_0)\, a_3\, (n / n_0)^{-1} \\ a_0, a_1, a_2, a_3 &= Const \end{aligned} \tag{65}$$

$$\text{Linear Scaling} : \Delta p > \Delta p_{max}$$
$$\dot{V} = \dot{V} - \underbrace{\frac{d\dot{V}}{dp}}_{Const} (\Delta p - \Delta p_{max})$$

$$\text{Logarithmic Scaling} : \left|\dot{V}\right| > \left|\dot{V}_{limit}\right|$$
$$V = \dot{V}_{limit} + K \ln(1 + (\dot{V} - \dot{V}_{limit})) , \dot{V} > \dot{V}_{limit}$$
$$\dot{V} = -\dot{V}_{limit} - K \ln(1 + \left|\dot{V} + V_{limit}\right|) , \dot{V} < -\dot{V}_{limit}$$

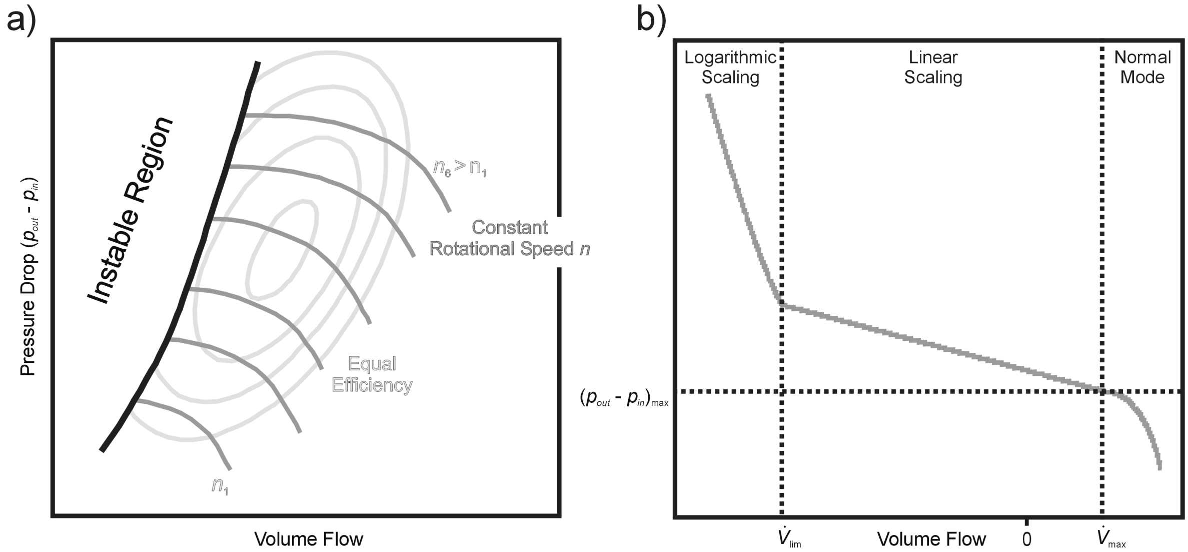

Figure 29: a) Characteristic map of a generalized fan
b) The different operation modes of the algorithm describing the generalized fan

The principal functioning of a fan has to be divided in two different modes (see Figure 30a). Within the ventilation mode ($p_{outlet} > p_{inlet}$) the air is pumped through the system. Within the flow resistance mode ($p_{inlet} > p_{outlet}$) the air is pushed through the fan. Inside the algorithm of the generalized fan these different modes doesn't be distinguished.

A specialized fan component is based on a measured characteristic map (see Figure 30a). The measured data set shows clearly the different operation modes of a fan. One Input (see Figure 28) is defined as inlet the other input is defined as outlet. Using the given pressure ratio (p_{outlet} / p_{inlet}) and a rotational speed n the corrected mass flow can be read out the measured characteristic map. Knowing $\dot{m}_{air,corr}$ the real mass flow $\dot{m}_{air}$ can be calculated with help of Equation 66.

$$\dot{m}_{air} = \dot{m}_{air,corr} \left(p_{inlet} / p_0\right) \frac{1}{\sqrt{T_{inlet} / T_0}} \qquad N = \frac{n}{\sqrt{T_{air,inlet} / T_0}} \tag{66}$$

p_0 and T_0 are pressure and temperature under ISA conditions. The corrected rotational speed N is a function of the real rotational speed n, T_0 and the inlet temperature under dry air conditions $T_{air,inlet}$ (see Equation 33).

Using $\dot{m}_{air,corr}$ the rise of temperature $\Delta T / T_{inlet}$ due to the compression of the fan can be determined (see Figure 30b). $\Delta T / T_{inlet}$ can be used to calculate the efficiency η_{fan}, the consumed power of the fan P_{fan} and the outlet temperature of the fan T_{outlet} (see Equation 67).

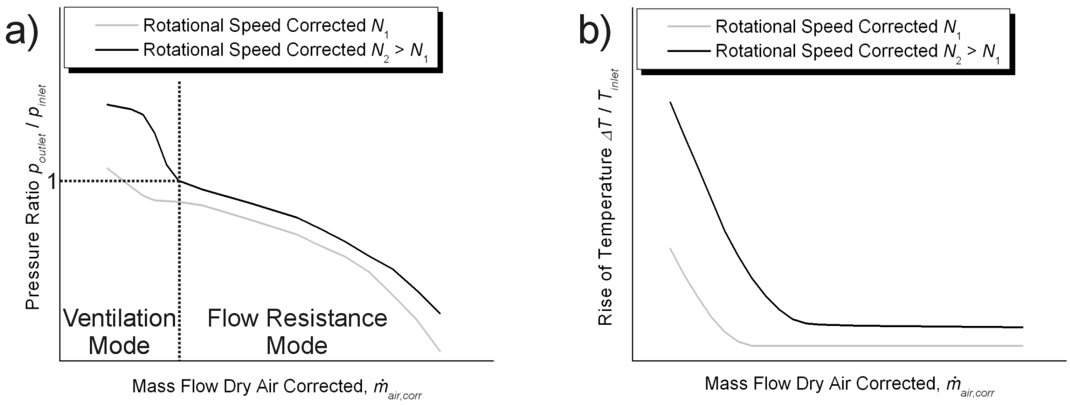

Figure 30: a) Characteristic map of a specialized fan
b) The rise of temperature describing the specialized fan

$$
\begin{aligned}
\eta_{fan} &= \frac{1}{\Delta T / T_{inlet}} \left(\left(\frac{p_{outlet}}{p_{inlet}}\right)^{\frac{\gamma - 1}{\gamma}} - 1 \right) \\
P_{fan} &= \frac{1}{\eta_{fan}} \dot{m}_{air} \, \bar{c}_p \, T_{inlet} \left(\left(\frac{p_{outlet}}{p_{inlet}}\right)^{\frac{\gamma - 1}{\gamma}} - 1 \right)
\end{aligned}
\tag{67}
$$

5.9 Turbine

Table 13: Input and output variables of a turbine

Input Variables	Output Variables
Pressure	Pressure
Density	Density
Temperature	Temperature
Water Vapor Content	Mass Flow Dry Air
CO_2 Content	Water Vapor Content
Water Content	CO_2 Content
	Water Content

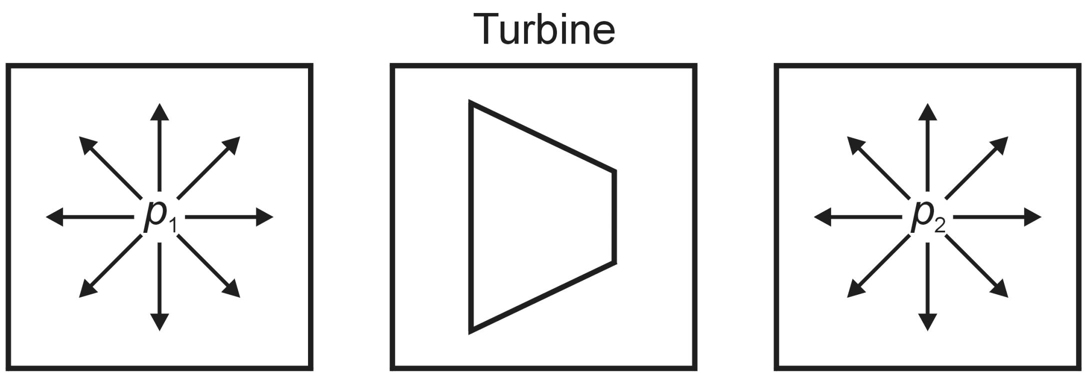

Figure 31: Configuration of a turbine as flow resistance

The turbine is defined as flow resistance (see Figure 30). Using the inlet pressure ratio p_{inlet} / p_{outlet} , $(p_{inlet} > p_{outlet})$ rotational speed n the mass flow $\dot{m}_{air}$ can be calculated (see Equation 68).

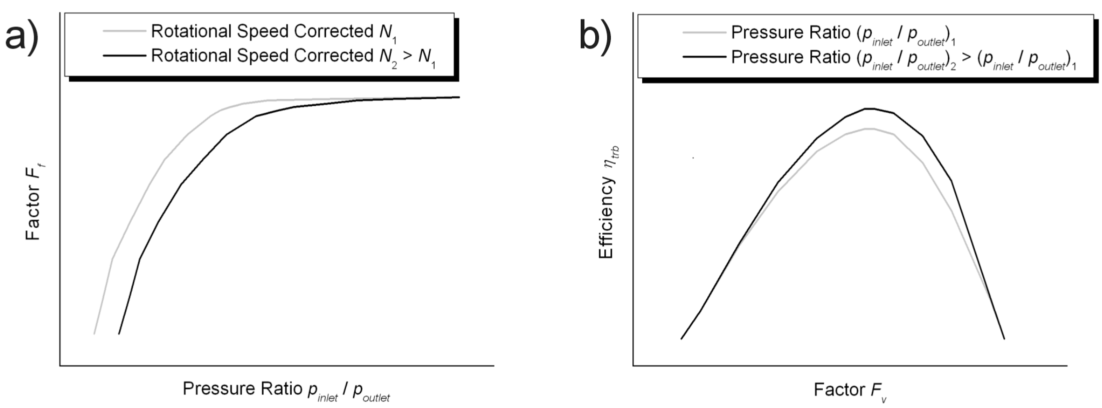

Figure 32: Characteristic maps of a turbine for the speed factor F_f and the isentropic efficiency η_{trb}

The rotational speed is projected onto the corrected value N (see Equation 66). Both the Mach number Ma and $\dot{m}_{air}$ are a function of the flow velocity v. To overcome the initialization problem the speed factor F_f has to be defined with help of a characteristic map (see Figure 32a, and Equation 68).

$$\dot{m}_{air}(v) = \frac{A\, p_{inlet}}{\sqrt{T_{inlet}}} \underbrace{\sqrt{\frac{\gamma}{R}}\, \mathrm{Ma}(v)\, (1 + \frac{\gamma - 1}{2} \mathrm{Ma}(v)^2)^{-\frac{\gamma+1}{2(\gamma-1)}}}_{F_f} \tag{68}$$

A is the effective Area of the turbine nozzle. Using the inlet temperature T_{inlet} and outlet temperature T_{outlet} the velocity factor F_v (see Equation 69) can be calculated. At a given pressure ratio with help of F_v the isentropic efficiency η_{trb} is defined (see Figure 32).

$$F_v = K \frac{n}{\sqrt{T_{inlet} - T_{outlet}}} \tag{69}$$

The constant K is valid for all turbines. With help of η_{trb} the outlet temperature can be calculated (see Equation 70). As a result of friction between air and turbine blades and condensation effects inside the turbine, the outlet temperature is higher than the theoretical outlet temperature. Due to this fact the isentropic efficiency underestimates the delivered power of the turbine P_{trb}. Determine P_{trb} the corrected isentropic efficiency η'_{trb} ($\eta'_{trb} = \eta_{trb} + \Delta\eta_{trb}$) has to be used.

$$\begin{aligned} T_{outlet} &= T_{inlet} - \eta_{trb}\, T_{inlet} \left(1 - (\frac{p_{outlet}}{p_{inlet}})^{\frac{\gamma-1}{\gamma}} \right) \\ P_{trb} &= \eta'_{trb}\, \dot{m}_{air}\, \bar{c}_p\, T_{inlet} \left(1 - (\frac{p_{outlet}}{p_{inlet}})^{\frac{\gamma-1}{\gamma}} \right) \end{aligned} \tag{70}$$

5.10 Compressor

Table 14: Input and output variables of a compressor

Input Variables	**Output Variables**
Pressure	Pressure
Density	Density
Temperature	Temperature
Water Vapor Content	Mass Flow Dry Air
CO_2 Content	Water Vapor Content
Water Content	CO_2 Content
	Water Content

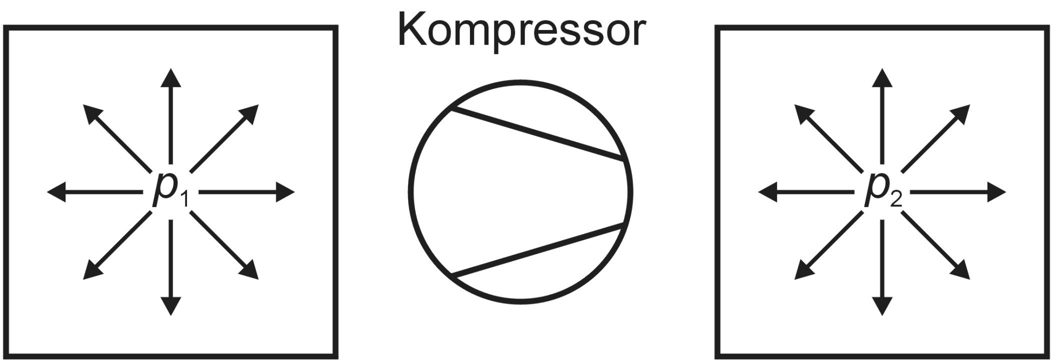

Figure 33: Configuration of a compressor as flow resistance

The compressor is treated as a flow resistance. In this setup the compressor is located between two pressure sources (see Figure 33).

By a given pressure ratio p_{outlet} / p_{inlet} and rotational speed n respectively N the mass flow through the compressor can be calculated with help of a characteristic map (see Figure 34a). Analogous to the fan component by a fixed rotational speed and pressure ratio theoretically the compressor achieves two possible mass flow values. In contrast to the fan component both values are possible solution.

Characteristic maps in the form of Figure 34a show an initialization problem. A priori the corresponding mass flow at given boundary limits respectively simulation setup aren't known. Determing the mass flow through the system, the compressor model has to work with a reference mass flow $\dot{m}_{ref}$. On the basis of $\dot{m}_{ref}$, it can be identified whether the compressor is working right hand side or left hand side of the mass flow $\dot{m}_{max}$. Under assumption of a fixed rotational speed $\dot{m}_{max}$ is the mass flow corresponding to the maximum pressure ratio.

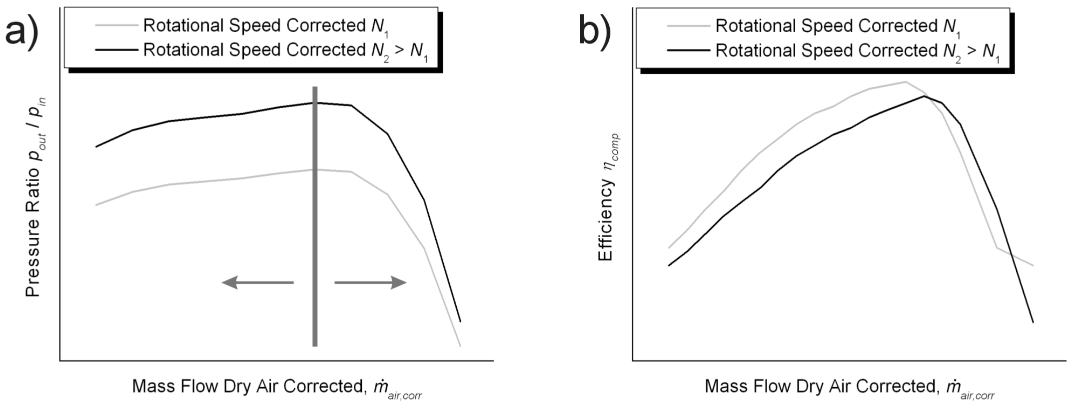

Figure 34: Characteristic maps of a compressor for the mass flow and the isentropic efficiency η_{comp}

Using the corrected mass flow respectively the real mass flow (see Equation 66) the isentropic efficiency η_{comp} (see Figure 34b) respectively the consumed power P_{comp} (see Equation 71) and the outlet temperature T_{outlet} can be calculated.

$$
\begin{aligned}
P_{comp} &= \frac{1}{\eta_{comp}} \dot{m}_{air} \, \bar{c}_p \, T_{inlet} \left(\left(\frac{p_{outlet}}{p_{inlet}}\right)^{\frac{\gamma - 1}{\gamma}} - 1 \right) \\
T_{outlet} &= T_{inlet} + \frac{1}{\eta_{comp}} T_{inlet} \left(\left(\frac{p_{outlet}}{p_{inlet}}\right)^{\frac{\gamma - 1}{\gamma}} - 1 \right)
\end{aligned}
\qquad (71)
$$

5.11 Vapor Cycle Air-Conditioning System

A common arrangement for the vapor compression system is shown in Figure 35. In vapor compression system having a compressor, a condenser, an expansion device and an evaporator arranged in succession and connected via a conduit in a closed loop for circulating refrigerant.

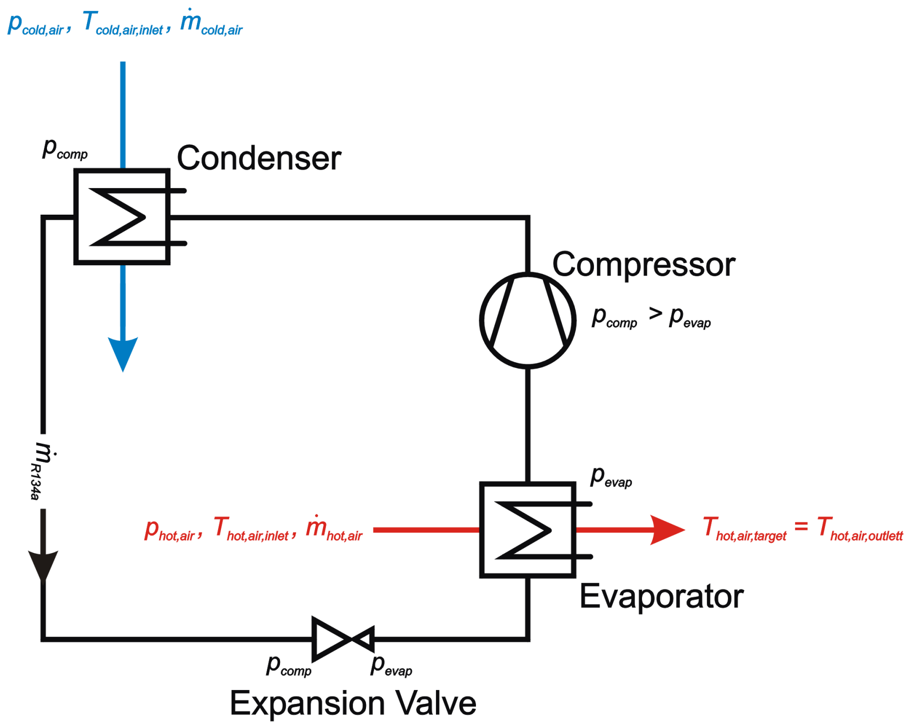

Figure 35: A common arrangement for the vapor compression system

Vapor compression cycle systems make use of the scientific fact that a liquid can be vaporized at any temperature by changing the pressure above it. Water at sea level barometric pressure of 101300 Pa will boil at 373.15 K = 100 °C. The same water in a closed tank under a pressure of 620532 Pa will not boil at less than 433.15 K = 160 °C. If the pressure is reduced to 6550 Pa by a vacuum pump, the water would boil at 311.15 K = 38 °C. Water can be made to boil at any temperature if the pressure corresponding to the desired boiling temperature can be maintained.

Liquids that boil at low temperatures are the most desirable for use as refrigerants. Comparatively large quantities of heat are absorbed when liquids are evaporated; that is, changed to a vapor. For this reason and reducing the ozone depletion potential, tetrafluoroethane R134a is used in most vapor cycle refrigeration units whether used in aircraft.

Refrigerant used in the vapor cycle system occurs as both a liquid and as a vapor. Conversion from a liquid to a vapor will occur at temperatures above -25 °C at sea level. If the refrigerant pressure is increased, conversion to a vapor will occur at higher temperatures. Maximum heat transfer efficiency occurs when the refrigerant is at the boiling point (the point at which the liquid will vaporize). The refrigerant must be delivered to the evaporator as a liquid if it is to absorb large quantities of heat. Since it leaves the evaporator in the form of a vapor, some way of condensing the vapor is necessary.

To condense the refrigerant vapor, the heat surrendered by the vapor during condensation must be transferred to some other medium. For this purpose, air is ordinarily used. The air must be at a temperature lower than the condensing temperature of the refrigerant. At any given pressure, the condensing and vaporizing temperatures of a fluid are the same. If a refrigerant that vaporizes at 5 °C is to be condensed at the same temperature, air at a lower temperature is needed. Obviously, if air at this lower temperature were available, mechanical refrigeration would not be required. As the temperature of available air is usually higher than the temperature of the boiling refrigerant in the evaporator, the refrigerant must be condensed after it leaves the evaporator.

To condense the vapor, its pressure must be increased to a point that its condensing temperature will be above the temperature of the air. For this purpose a compressor is needed. After the pressure of the refrigerant vapor has been increased sufficiently, it may be liquefied in the condenser with comparatively warm air (ISA Hot Day). In a practical refrigeration circuit, liquid flows from the condenser to the expansion valve, which is essentially nothing more than a needle valve. The compressor maintains a difference in pressure between the evaporator and the condenser. Without the expansion valve, this difference in pressure could not be maintained. The expansion valve separates the high-pressure part of the system from the low-pressure part. Only a small trickle of refrigerant fluid flows through the valve into the evaporator. The valve is always adjusted so that only the amount of liquid that can be vaporized in the evaporator passes through it. The liquid that flows through the evaporator is entirely vaporized by the heat flowing through the walls of the evaporator. A receiver acts as a reservoir for the R134a refrigerant. The fluid level in the receiver varies with system demands. During peak cooling periods, there will be less liquid than when the load is light. The purpose of the receiver is to ensure that the thermostatic expansion valve is not starved for refrigerant under heavy cooling load conditions.

Refrigerant Criteria:

- **Chemical:**
  - Stable and inert
- **Health, safety and environmental:**
  - Non-toxic
  - Non-flammable
  - Benign to the atmosphere etc
- **Thermal:**
  - Critical point and boiling point temperatures appropriate for the application
  - Low vapor heat capacity
  - Low viscosity
  - High thermal conductivity
- **Other:**
  - Satisfactory oil solubility/miscibility
  - High dielectric strength of vapor
  - Low freezing point
  - Reasonable containment materials
  - Easy leak detection
  - Low cost

Refrigeration Cycle: A standard vapor compression cycle composed mainly of four main equipments: Evaporator, Compressor, Condenser and a throttling valve as illustrated in Figure 35, while Figure 36 shows the corresponding *p-h*, *T-s* respectively *T-h* diagrams.

The following assumptions are made

- An evaporation at constant pressure, in the evaporator with an evaporator temperature, T_{evap}, from point 4 to point 1 (h_4 to h_1): $\dot{Q}_{evap} = \dot{m}_{R134a}\,(h_1 - h_4)$.
- An adiabatic isentropic compression process in the compressor, corresponding from point 1 to point 2 (h_1 to h_2): $P_{comp} = \dot{m}_{R134a}\,(h_2 - h_1)$.
- The superheating followed by a condensation at constant temperature T_{cond} and pressure p_{comp} in the condenser, from point 2 to point 3 (h_2 to h_3): $\dot{Q}_{cond} = \dot{m}_{R134a}\,(h_2 - h_3)$.
- An expansion at constant enthalpy in the throttling valve, corresponding from point 3 to point 4 ($h_3 = h_4$): $\dot{m}_{R134a}\,(h_3 - h_4) = 0$.
- The vapor leaving the evaporator as well as the liquid leaving the condenser are supposed to be at least at saturated states. In the general case the vapor are superheated and the liquid are subcooled.

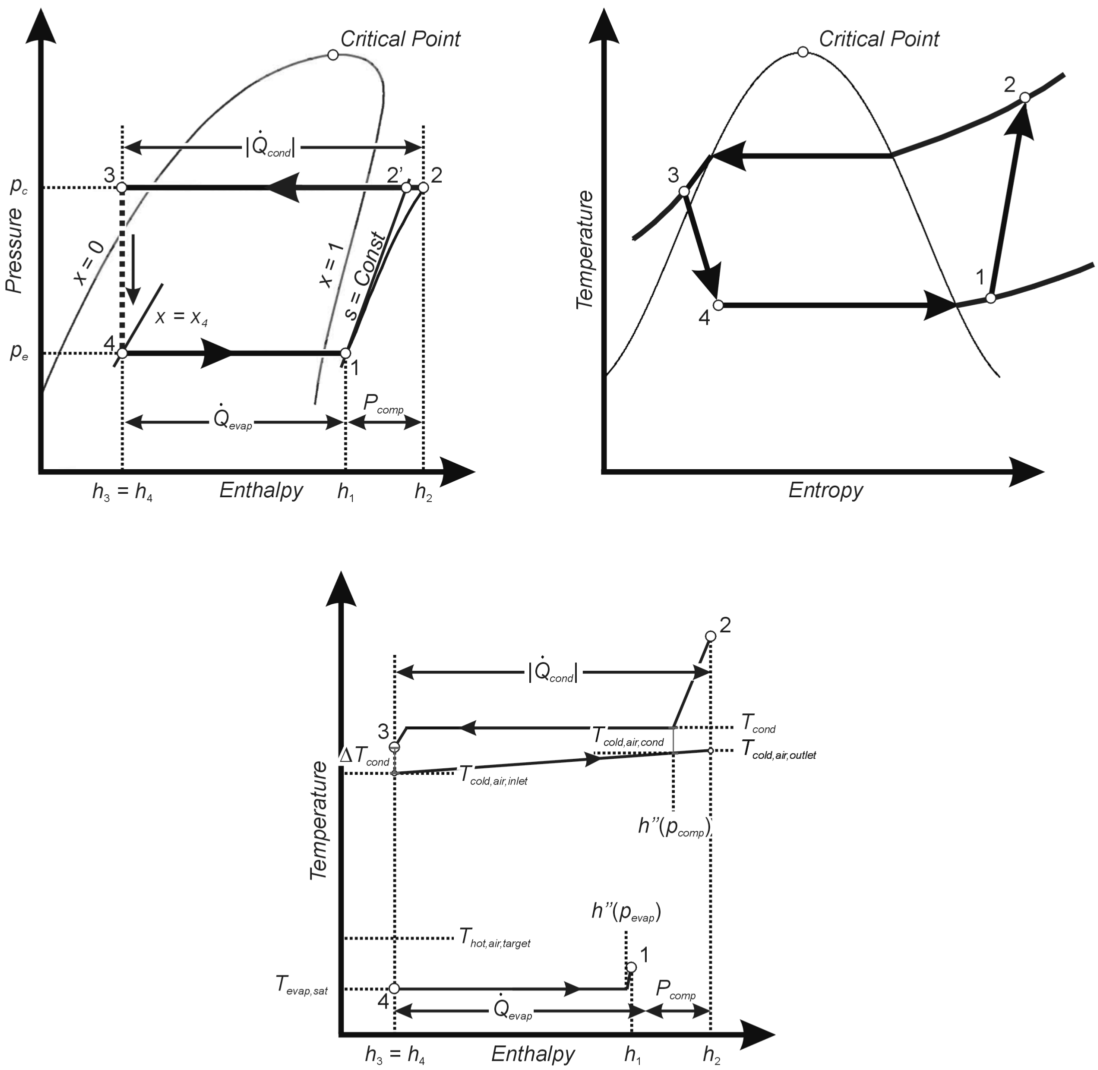

Figure 36: *p-h*, *T-s* respectively *T-h* diagrams of R134a refrigerant

Inside the Simulation model the physical and thermodynamics properties of the refrigerant are fixed by characteristic maps. A important characteristc map (see Figure 37) i s the enthalpy as function of pressure and temperature ($h = f(p,T)$) . Additionally (see Figure 37) the saturation pressure p_{sat} at a given temperature T_{sat} ($p_{sat} = f(T_{sat})$) and the enthalpy functions $h' = f(p_{sat}) = g(T_{sat})$ (boiling line: $x = 0$) and $h'' = f(p_{sat}) = g(T_{sat})$ (dewing line: $x = 1$) have to be known.

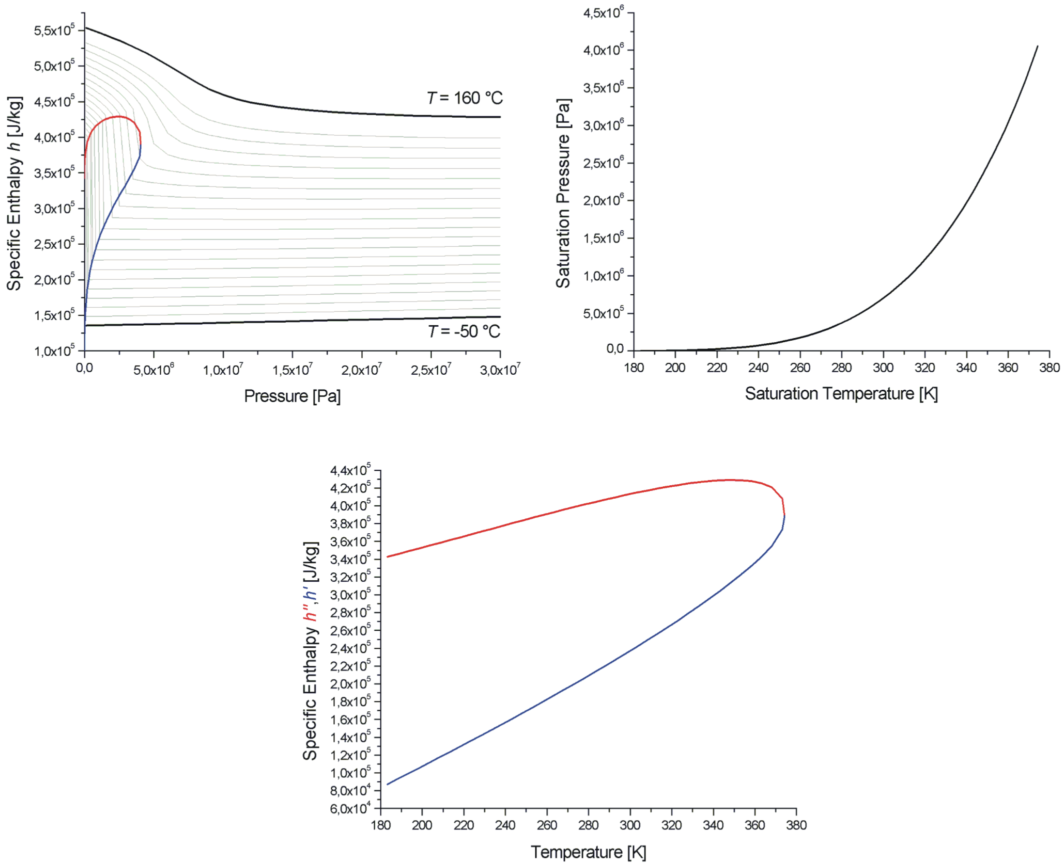

Figure 37: Characteristic maps of a vapor compression cycle model

According to the assumption the components of a vapor compression cycle model require certain set of input and out variables (see Table 15). The inner structure of the algorithm will be discussed in TN_APP.

Table 15: Input and output variables of a component inside a vapor compression cycle model

Input Variables	Output Variables
Pressure	Pressure
Enthalpy	Enthalpy, Inlet
Temperature	Enthalpy, Outlet
Mass Flow	Temperature, Inlet
	Temperature, Outlet
	Mass Flow

Bibliography

Allied-Signal 1990 Allied-Signal Aerospace Company, Inc.: Airesearch Enviromental Control System: An Overview. Los Angeles : 1990. – Presentation

Baehr 1995 BAEHR, Hans Dieter; TILLNER-ROTH, Reiner: *Thermodynamische Eigenschaften umweltverträglicher Kältemittel*. Berlin : Springer. 1995

Baehr 2006 BAEHR, Hans Dieter: *Thermodynamik*. Berlin : Springer. 2006

Böswirth 2000 BÖSWIRTH, Leopold: *Technische Strömungslehre*. Wiesbaden : Vieweg, 2000

Bohl 1998 BOHL, Willi: *Technische Strömungslehre* : *Stoffeigenschaften von Flüssigkeiten und Gasen, Hydrostatik, Aerostatik, Inkompressible Strömungen, Kompressible Strömungen, Strömungsmeßtechnik*. Würzburg : Vogel, 1998

Chawla 1990 CHAWLA, J. M.; WISKOT, G.: *Wärmeübertragung* : *Berechnung mit dem PC*. Düsseldorf : VDI, 1992

Eichholz 2005 EICHHOLZ, J.; Airbus Deutschland GmbH, EYVCG : Standardization of Simulation Models in EYV. Hamburg : Airbus, 2005 (EYVC048/05). – Firmenschrift

Gupta 1998 GUPTA, J. Y.: *Fundamentals of Heat Exchanger and Pressure Vessel Technology*. New York : Hemisphere Publishing Corporation, 1985

Herwig 2004 HERWIG, Heinz: *Strömungsmechanik* : *Eine Systematische Einordnungvon Begriffen und Konzepten der Strömungsmechanik*. Wiesbaden : Vieweg, 2004

Incropera 2003 INCROPERA, FRANK P.; DEWITT, DAVID P.: *Fundamentals of Heat and Mass Transfer*. New York : John Wiley & Sons, 2002

Idel'chik 1994 IDEL'CHIK, L. E.: *Handbook of Hydraulik Resistance*. Boca Raton : CRC Press, 1994

Mishra 2004 MISHRA, Manish; DAS, P.K.; SARANG, Sunil: Transient behaviour of crossflow heat exchangers with longitudinal conduction and axial dispersion. In: *International Journal of Heat Transfer*, Vol. 126 (2004), No. 3, pp. 425-433

Mishra 2006 MISHRA, Manish; DAS, P.K.; SARANG, Sunil: Transient behaviour of crossflow heat exchangers due to perturbations in temperature and flow. In: *International Journal of Heat and Mass Transfer*, Vol. 49 (2006), Issues 5-6, pp. 1083-1089

Patankar 1980 PATANKAR, Suhas V.: *Numerical heat transfer and fluid flow*. Pristol, PA : Taylor & Francis, 1980

Podhorsky 1990 PODHORSKY, M.; KRIPS, H.: *Wärmetauscher* : *Allgemeine Probleme der Konstruktion und Berechnung*. Essen : Vulkan, 1990 (FDBR-Fachbuchreihe, Band 5)

Roetzel 1998 ROETZEL, Wilfried; XUAN, Yimin: *Dynamic Behaviour of Heat Exchanger*. Southhampton : WitPress, 1999 (Developments in Heat Transfer, Vol. 3)

Scholz 1999 SCHOLZ, Dieter: *Entwicklung eines CAE- Werkzeuges zum Entwurf von Flugsteuerungs- und Hydrauliksystemen*. Düsseldorf : VDI, 1997 (Fortschritt-Berichte VDI, Reihe 20, Nr. 262)

Shah 2003 SHAH, Ramesh K.; SEKULIĆ, Dušan P.: *Fundamentals of Heat Exchanger Design*. New York : John Wiley & Sons, 2003

Thoma 2000 THOMA, J.; OULD BOUAMANA, B.: *Modelling and Simulation in Thermal and Chemical Engineering* : *A Bond Graph Approach*. Berlin : Springer, 2000

VDI 2002 VEREIN DEUTSCHER INGENIEURE (Hrsg.): *VDI-Wärmeatlas* : *Berechnungsblätter für den Wärmeübergang*. Berlin : Springer, 2002

Wagner 1998 WAGNER, Walter: *Wärmetauscher* : *Grundlagen, Aufbau und Funktion Thermischer Apparate*. Würzburg : Vogel, 1993

Wesseling 2000 WESSELING, Pieter: *Principles of Computational Fluid Dynamics*. Springer : Berlin, 2000

Wylie 1993 WYLIE, E. B.; STREETER, V. L.: *Fluid Transients in Systems*. Englewood : Printice-Hall, 1993